

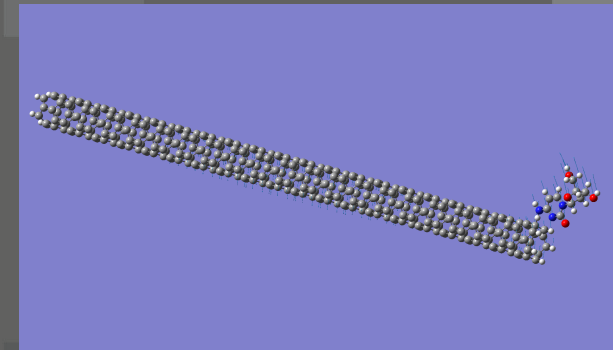
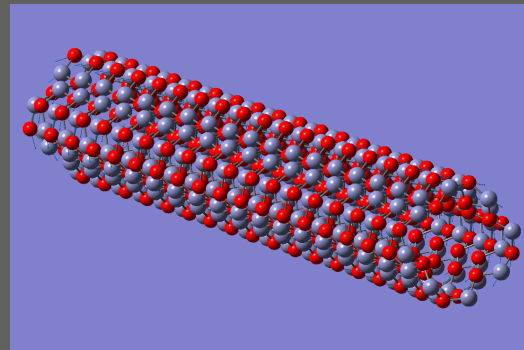
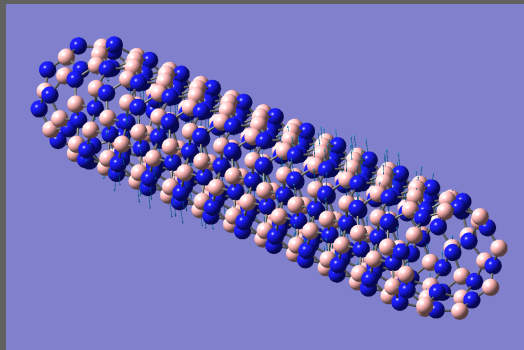


Swansea University
Prifysgol Abertawe

Atomistic Mechanics of Nanoscale Structures: Static & Dynamic Analyses

Sondipon Adhikari

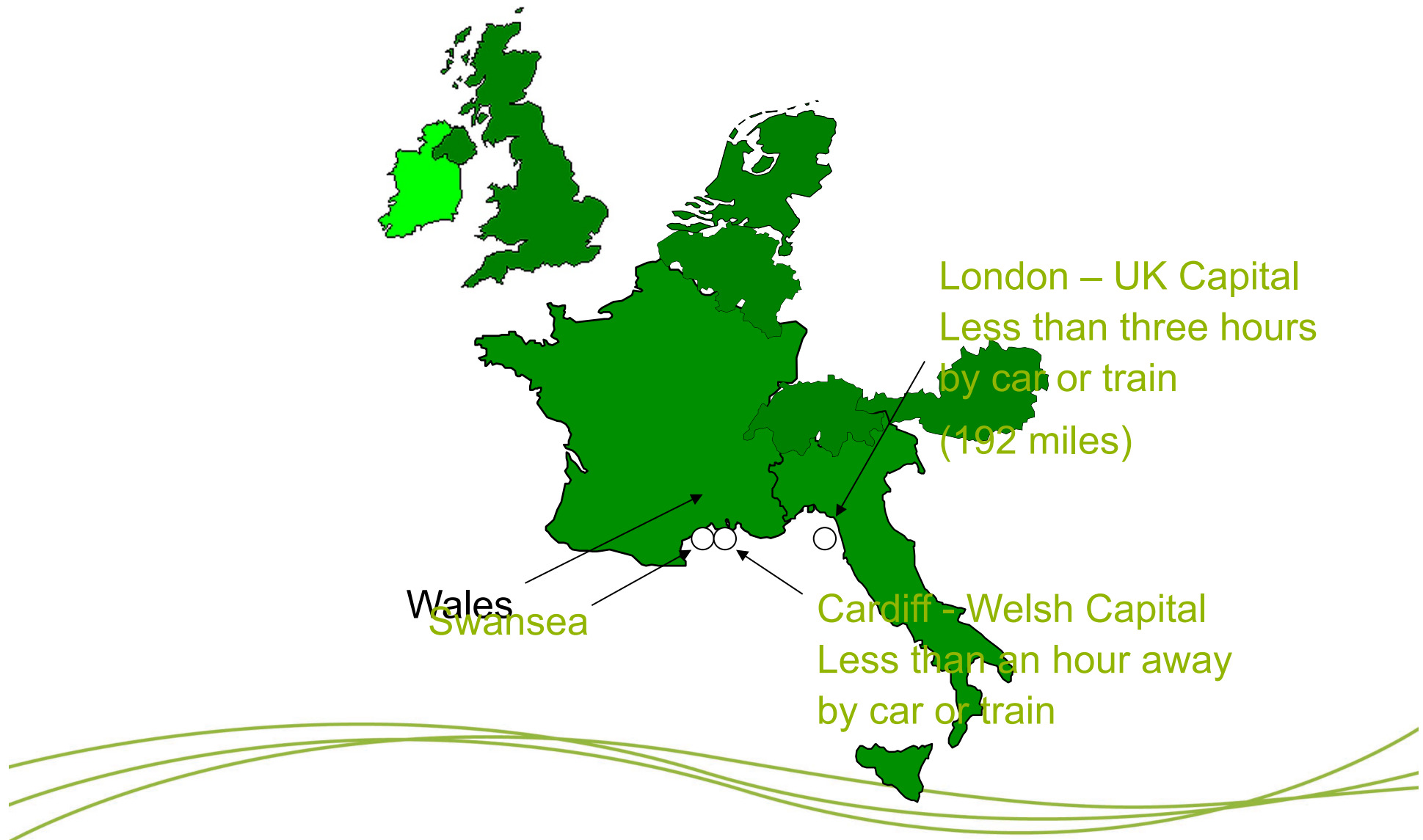
IISc Bangalore
13 January 2012

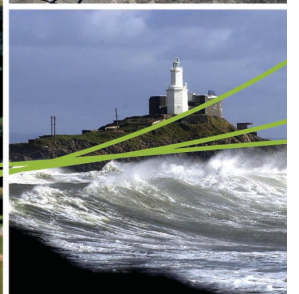


Where is Swansea?



Swansea University
Prifysgol Abertawe





Swansea University



Swansea University
Prifysgol Abertawe



- 29th UK university to be established
- King George V laid the foundation stone of the University in July 1920
- Now over 12,500 students - 1,800 international



Overview

- Introduction
- Atomistic finite element method
- Carbon nanotubes: static and dynamic analysis, buckling
- Fullerenes: vibration spectra
- Graphene: static and dynamic analysis, composites
- Nanobio sensors: vibrating nanotube and graphene based mass sensor
- DNA mechanics
- Conclusions



Research Areas

- ◆ Atomistic finite element method
- ◆ Nonlocal continuum mechanics for nanoscale objects
- ◆ Nanoscale bio sensors
- ◆ Uncertainty quantification in modelling and simulation
- ◆ Dynamic analysis of complex structures
- ◆ Vibration energy harvesting



Collaborators

- ◆ Prof F Scarpa (University of Bristol)
- ◆ Dr R Chowdhury, Dr C Wang, Dr A Gil, Prof P Rees (Swansea University).
- ◆ Dr T Murmu, Prof M McCarthy (University of Limerick)

Acknowledgements



EPSRC

Pioneering research
and skills



Swansea University
Prifysgol Abertawe





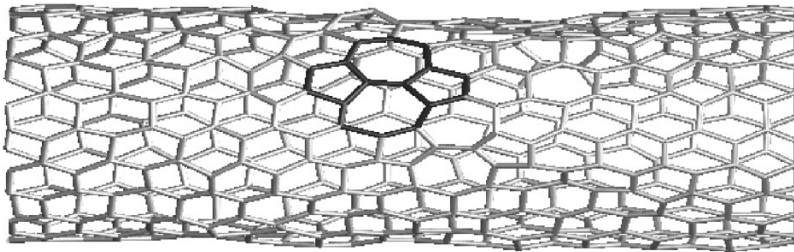
Swansea University
Prifysgol Abertawe

Carbon Nanotubes

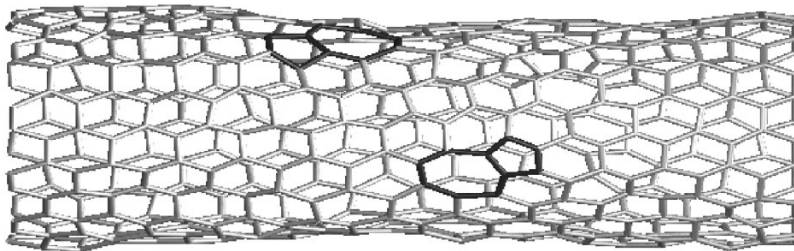


Can we use continuum mechanics at the nanoscale?

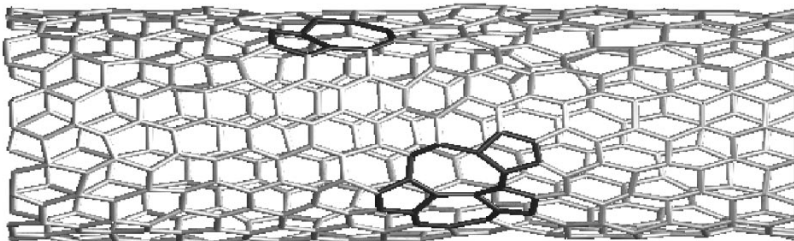
a)



b)



c)

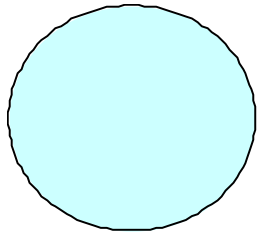


- ◆ What about the “holes”?
- ◆ Can we have an “equivalent” continuum model with “correct” properties?
- ◆ How defects can be taken into account ?



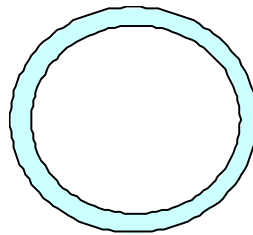
Which Young's modulus?

Effective



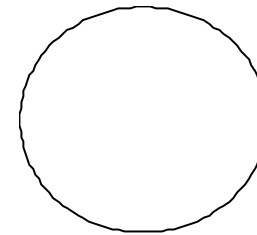
$$\bar{Y}_{11} = \frac{F}{\pi R^2 \epsilon_{11}}$$

Longitudinal



$$Y_{11} = \frac{F}{2\pi R d \epsilon_{11}}$$

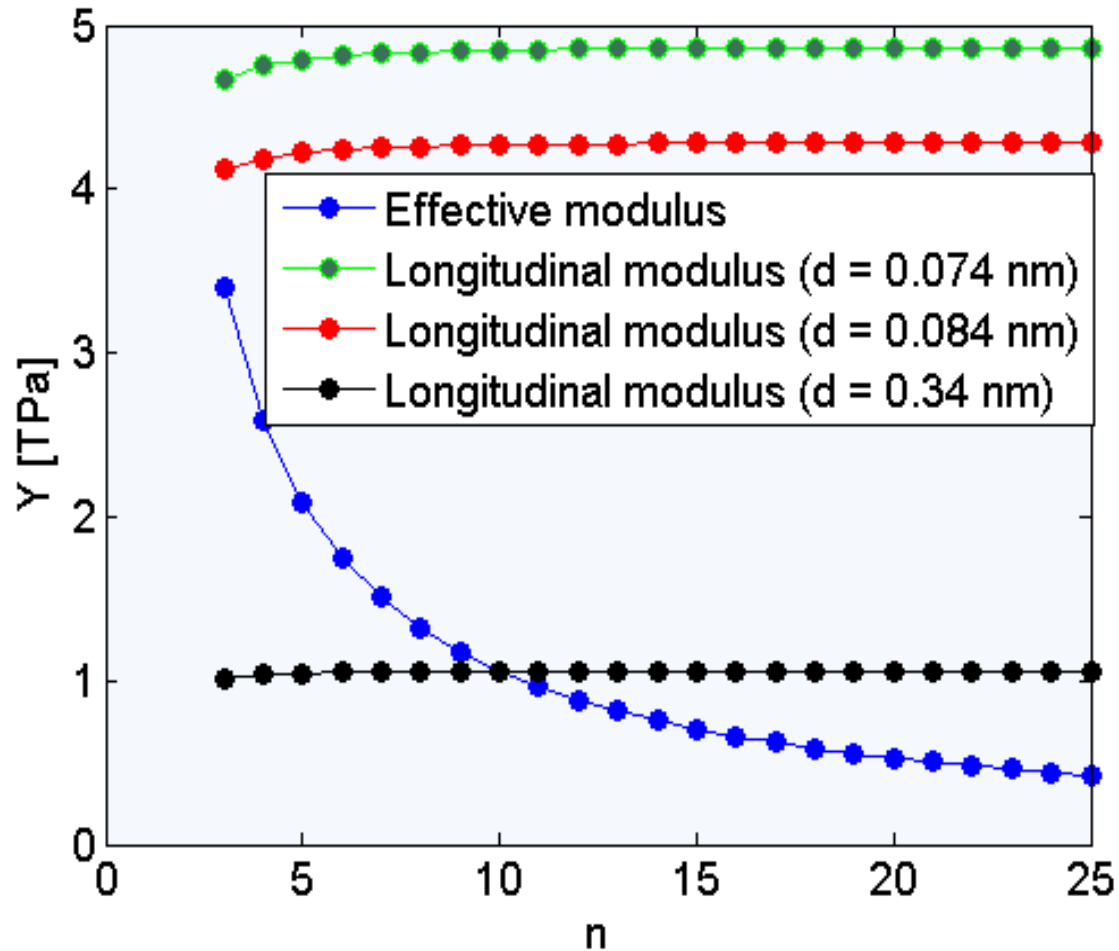
Surface



$$Y_{11}^s = \frac{F}{2\pi R \epsilon_{11}}$$



Which Young's modulus?





Yakobson's paradox

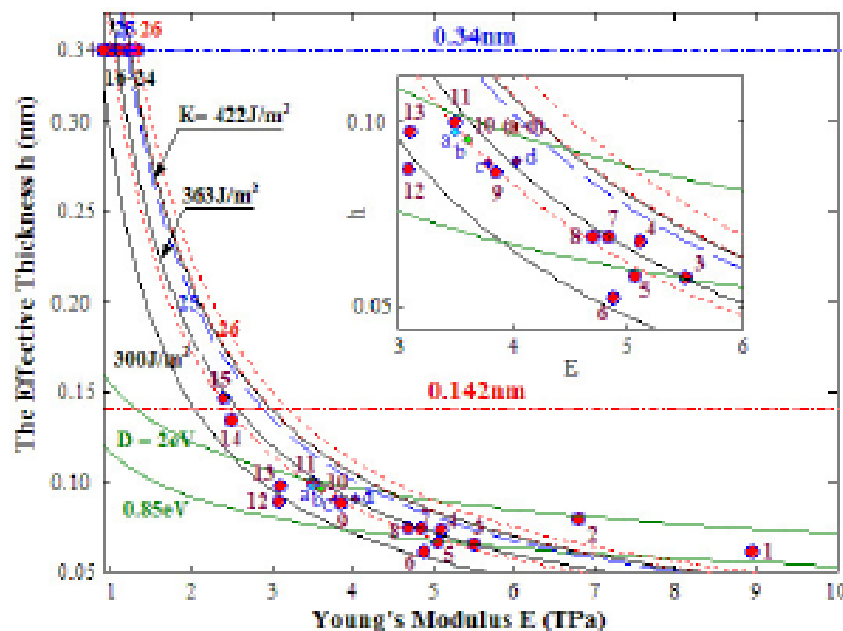


Figure 1. The effective thickness h , Young's modulus E , in-plane stiffness $K = \frac{Eh}{1-\nu^2} \approx Eh$ and the bending stiffness $D = \frac{Eh^3}{12(1-\nu^2)}$ obtained in the literature for SWCNTs, where ν is Poisson's ratio. Among the five solid lines two represent bending stiffness $D = \frac{Eh^3}{12(1-\nu^2)} \approx \frac{Eh^3}{12} = 0.85 \text{ eV}$ and 2 eV , respectively. The other three solid lines are associated with increasing in-plane stiffness $K = \frac{Eh}{1-\nu^2} \approx Eh = 300, 360$ and 422 J m^{-2} . Dots 10(a-d) are given by [9]. The models and sources of the dots in the figure are listed in table 1.

Authors	Method	Wall thickness (nm)	Young's modulus (TPa)
Lu ^a	Molecular dynamics	0.34	0.974
Hernández <i>et al.</i> ^b	Tight binding molecular dynamics	0.34	1.24
Odegard <i>et al.</i> ^c	Equivalent-continuum modeling	0.69	
Li and Chou ^d	Structural mechanics: stiffness matrix method	0.34	1.01
Jin and Yuan ^e	Molecular dynamics	0.34	1.238
Tserpes and Papanikos ^f	Structural mechanics: FE method	0.147	
Yakobson <i>et al.</i> ^g	Molecular dynamics	0.066	5.5
Zhou <i>et al.</i> ^h	Tight-binding model	0.074	5.1
Kudin <i>et al.</i> ⁱ	<i>Ab initio</i> computations	0.089	3.859
Tu and Ou-yang ^j	Local density approximation model	0.075	4.7
Vodenitcharova and Zhang ^k	Ring theory continuum mechanics	0.0617	4.88
Panatano <i>et al.</i> ^l	Continuum shell modeling	0.075	4.84
Goupalov ^m	Continuum model for long-wavelength phonons	0.087	
Wang <i>et al.</i> ⁿ	<i>Ab initio</i> calculation	0.0665	5.07

(Wang CY, Zhang LC, 2008. *Nanotechnology* 19, 075705)
(Huang Y, Wu J, Hwang K C, 2006. *Phys. Rev. B* 74, 245413)



Atomistic finite element method

- ◆ Atomic bonds are represented by beam elements
- ◆ Beam properties are obtained by energy balance

$$U_{total} = U_r + U_\theta + U_\tau$$

$$U_r = \frac{1}{2}k_r(\Delta r)^2 \quad U_\theta = \frac{1}{2}k_\theta(\Delta\theta)^2 \quad U_\tau = \frac{1}{2}k_\tau(\Delta\phi)^2$$

$$U_{axial} = \frac{1}{2}K_{axial}(\Delta L)^2 = \frac{EA}{2L}(\Delta L)^2$$

$$U_{torsion} = \frac{1}{2}K_{torsion}(\Delta\beta)^2 = \frac{GJ}{2L}(\Delta\beta)^2$$

$$U_{bending} = \frac{1}{2}K_{bending}(2\alpha)^2 = \frac{EI}{2L} \frac{4+\Phi}{1+\Phi} (2\alpha)^2$$

Scarpa, F. and Adhikari, S., "A mechanical equivalence for the Poisson's ratio and thickness of C-C bonds in single wall carbon nanotubes", Journal of Physics D: Applied Physics, 41 (2008) 085306



Atomistic finite element method

◆ All parameters of the beam can be obtained in closed-form:

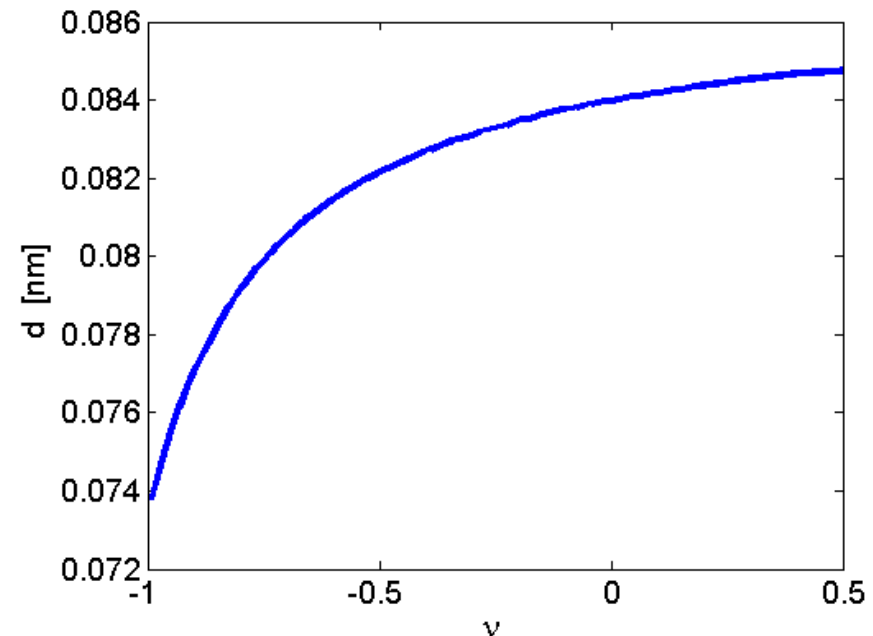
$$E = \frac{4k_r L}{\pi d^2}, \quad G = \frac{32k_r L}{\pi d^4}$$

$$\Phi = \frac{3k_r d^4 (6 + 12\nu + 6\nu^2)}{32k_r L^2 (7 + 12\nu + 4\nu^2)}$$

$$k_\theta = \frac{k_r d^2}{16} \frac{4A + B}{A + B} \quad d < 2\sqrt{6} \sqrt{\frac{k_r}{k_r}}$$

$$A = 112L^2 k_r + 192L^2 k_r \nu + 64L^2 k_r \nu^2$$

$$B = 9k_r d^4 + 18k_r d^4 \nu + 9k_r d^4 \nu^2$$



Scarpa, F. and Adhikari, S., "A mechanical equivalence for the Poisson's ratio and thickness of C-C bonds in single wall carbon nanotubes", Journal of Physics D: Applied Physics, 41 (2008) 085306

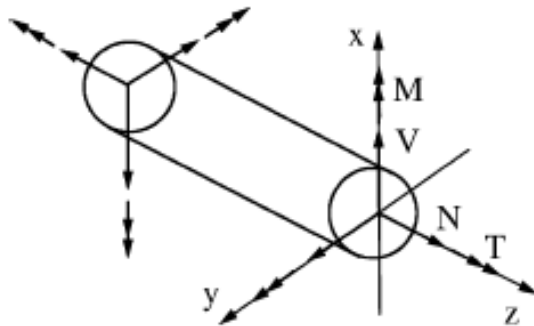


Atomistic Structural Mechanics

For space frames:

$$[\mathbf{K}]\{\mathbf{u}\} = \{\mathbf{f}\}$$

$[\mathbf{K}] \rightarrow$ stiffness matrix
 $\{\mathbf{u}\} \rightarrow$ nodal displacement vector
 $\{\mathbf{f}\} \rightarrow$ nodal force vector



$$\mathbf{u} = [u_{xi}, u_{yi}, u_{zi}, \theta_{xi}, \theta_{yi}, \theta_{zi}, u_{xj}, u_{yj}, u_{zj}, \theta_{xj}, \theta_{yj}, \theta_{zj}]^T$$

$$\mathbf{f} = [f_{xi}, f_{yi}, f_{zi}, m_{xi}, m_{yi}, m_{zi}, f_{xj}, f_{yj}, f_{zj}, m_{xj}, m_{yj}, m_{zj}]^T$$

$$\mathbf{K} = \begin{bmatrix} \mathbf{K}_{ii} & \mathbf{K}_{ij} \\ \mathbf{K}_{ij}^T & \mathbf{K}_{jj} \end{bmatrix}$$

$$\mathbf{K}_{ii} = \begin{bmatrix} EA/L & 0 & 0 & 0 & 0 & 0 \\ 0 & 12EI_x/L^3 & 0 & 0 & 0 & 6EI_x/L^2 \\ 0 & 0 & 12EI_y/L^3 & 0 & -6EI_y/L^2 & 0 \\ 0 & 0 & 0 & GJ/L & 0 & 0 \\ 0 & 0 & -6EI_y/L^2 & 0 & 4EI_y/L & 0 \\ 0 & 6EI_x/L^2 & 0 & 0 & 0 & 4EI_x/L \end{bmatrix}$$

$$\mathbf{K}_{ij} = \begin{bmatrix} -EA/L & 0 & 0 & 0 & 0 & 0 \\ 0 & -12EI_x/L^3 & 0 & 0 & 0 & 6EI_x/L^2 \\ 0 & 0 & -12EI_y/L^3 & 0 & -6EI_y/L^2 & 0 \\ 0 & 0 & 0 & -GJ/L & 0 & 0 \\ 0 & 0 & 6EI_y/L^2 & 0 & 2EI_y/L & 0 \\ 0 & -6EI_x/L^2 & 0 & 0 & 0 & 2EI_x/L \end{bmatrix}$$

(Weaver Jr., W. and Gere, J.M., 1990. Matrix Analysis of Framed Structures. (third ed.), Van Nostrand Reinhold, New York)

$$\mathbf{K}_{jj} = \begin{bmatrix} EA/L & 0 & 0 & 0 & 0 & 0 \\ 0 & 12EI_x/L^3 & 0 & 0 & 0 & -6EI_x/L^2 \\ 0 & 0 & 12EI_y/L^3 & 0 & 6EI_y/L^2 & 0 \\ 0 & 0 & 0 & GJ/L & 0 & 0 \\ 0 & 0 & 6EI_y/L^2 & 0 & 4EI_y/L & 0 \\ 0 & -6EI_x/L^2 & 0 & 0 & 0 & 4EI_x/L \end{bmatrix}$$



Atomistic FE – bending deformation of SWCNTs

Table 2. Bending modulus, thickness and Poisson's ratio for zigzag and armchair SWCNTs. Aspect ratio (tube length/tube diameter) is 20.

Radius (nm)	ν	d (nm)	E (TPa)	G (TPa)	Y_f (TPa)	ϵ_f
<i>Zigzag</i>						
0.378	0.0344	0.112	16.79	2.54	0.88	3.51×10^{-5}
0.777	0.0344	0.0853	16.77	7.61	1.078	1.84×10^{-5}
0.935	0.0344	0.0842	16.65	8.02	1.079	1.56×10^{-5}
1.1708	0.0344	0.0837	16.81	8.17	1.083	1.24×10^{-5}
<i>Armchair</i>						
0.246	0.0344	0.0773	19.7	11.25	2.7	2.51×10^{-5}
0.585	0.0344	0.0911	14.22	5.85	1.26	1.935×10^{-5}
0.883	0.0344	0.0841	16.65	8.02	1.15	1.54×10^{-5}
1.312	0.0344	0.0836	16.89	8.25	1.075	1.12×10^{-5}

(F Scarpa and S Adhikari, 2008. *J. Phys. D: App. Phys.*, 41, 085306)

Atomistic FE – bending deformation of SWCNTs bundles

Similarity between hexagonal SWCNT packing bundle and structural idealization for wing boxes

Polar moment of inertia for each CNT:

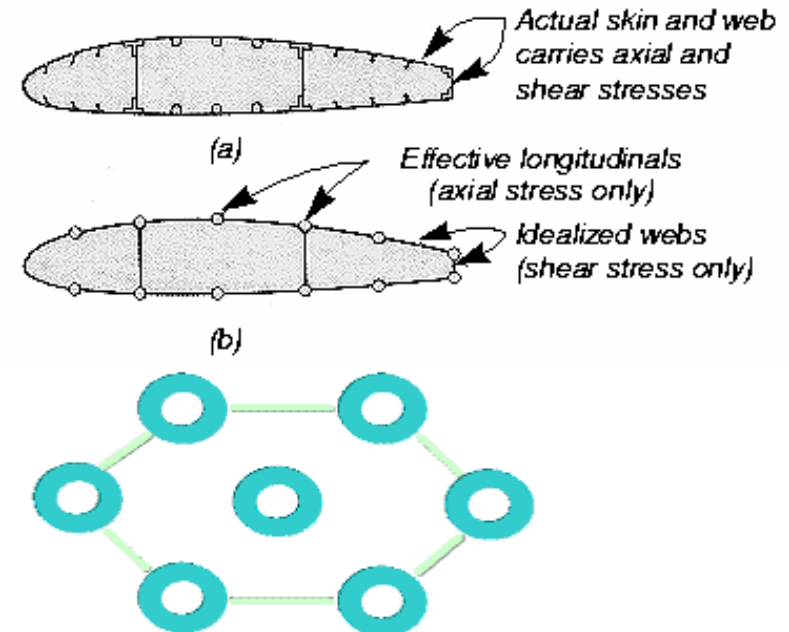
$$I_c = \frac{\pi}{4} \left[\left(R + \frac{d}{2} \right)^4 - \left(R - \frac{d}{2} \right)^4 \right] \quad (1)$$

Polar moment of inertia for hexagonal packing:

$$I_{hex} = 4 \left(I_c + \left(3 \frac{l_0^2}{2} \right)^2 A_c \right) + 3I_c \quad (2)$$

Flexural modulus of the nanbundle:

$$\bar{Y}_f = Y \frac{I_{hex}}{I_h} \quad (3)$$

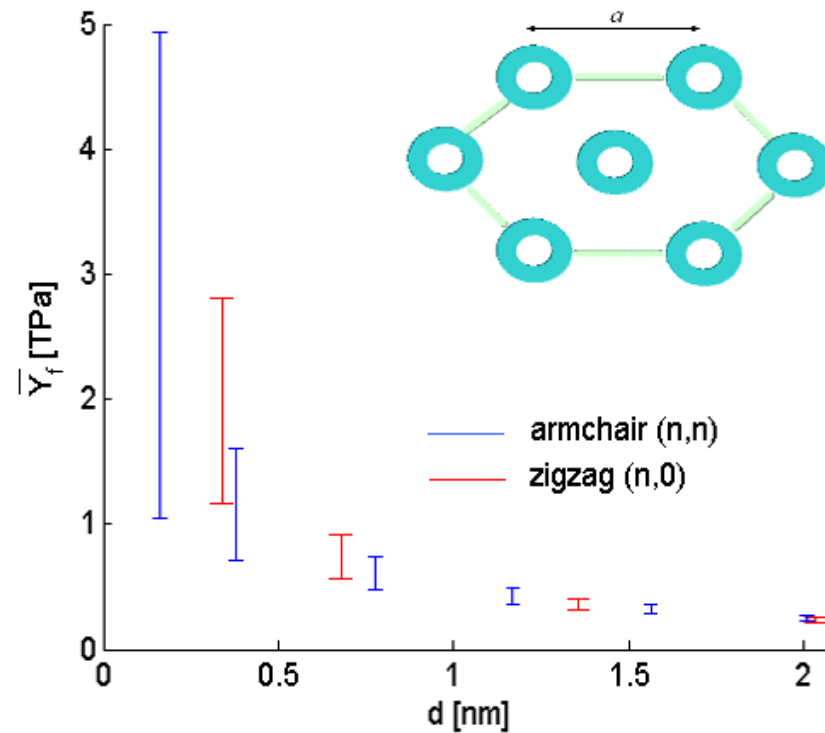


$$\bar{Y}_f = Y \left[\frac{20\sqrt{3}\pi R^3 d}{3(2R + t_{vdw})^4} + \frac{7\sqrt{3}\pi R d^3}{33(2R + t_{vdw})^4} + \frac{64\sqrt{3}\pi R^2 t_{vdw} d}{11(2R + t_{vdw})^4} + \frac{16\sqrt{3}\pi R t_{vdw}^2 d}{11(2R + t_{vdw})^4} \right]$$

(F Scarpa and S Adhikari, 2008. *J. Phys. D: App. Phys.*, 41, 085306)



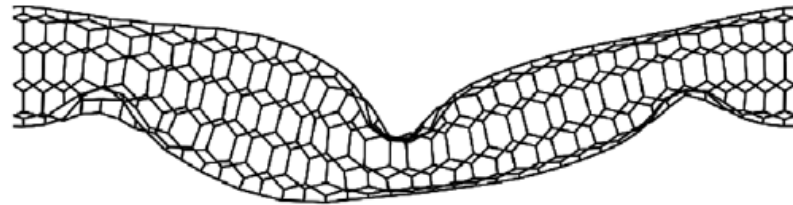
Atomistic FE – bending deformation of SWCNTs bundles



(F Scarpa and S Adhikari, 2008. *J. Phys. D: App. Phys.*, 41, 085306)



Buckling of Carbon nanotubes

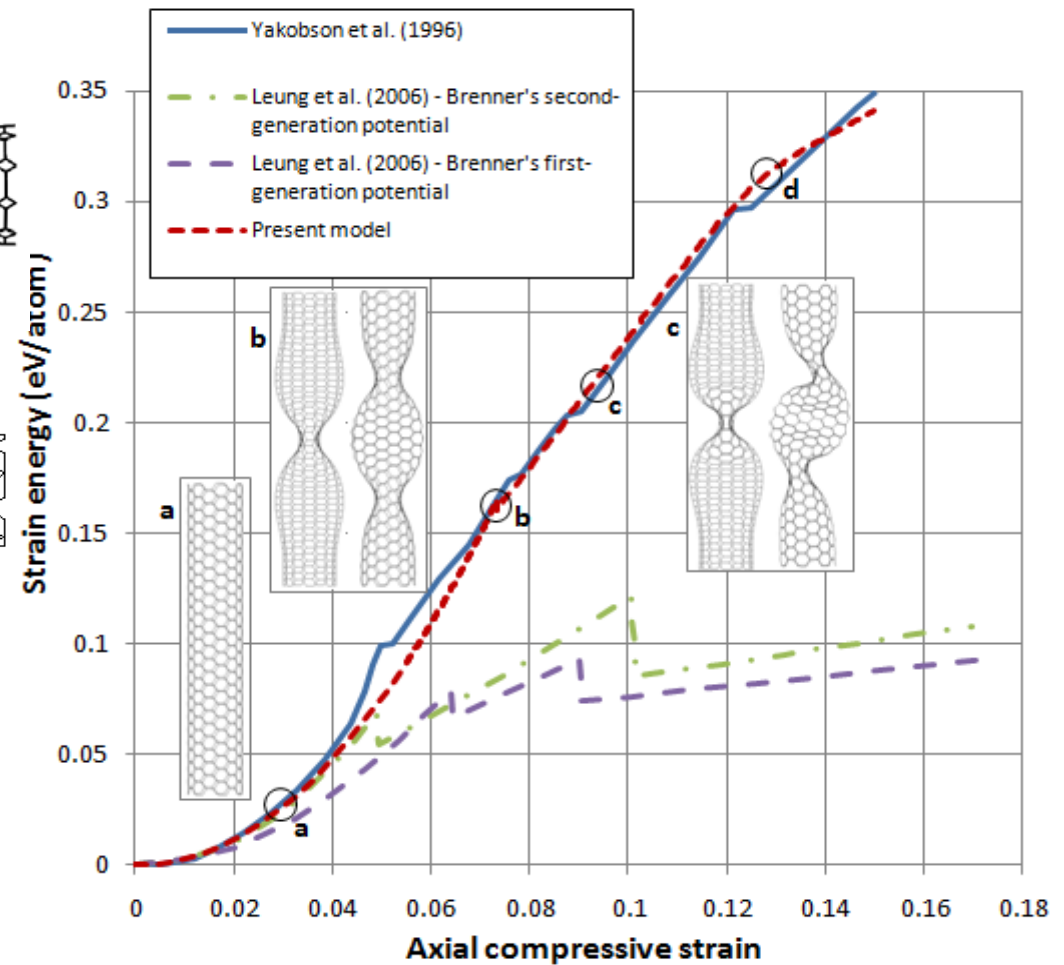


(a) Molecular dynamics



(b) Hyperelastic atomistic FE (Ogden strain energy density function)

Comparison of buckling mechanisms in a (5,5) SWCNT with 5.0 nm length.

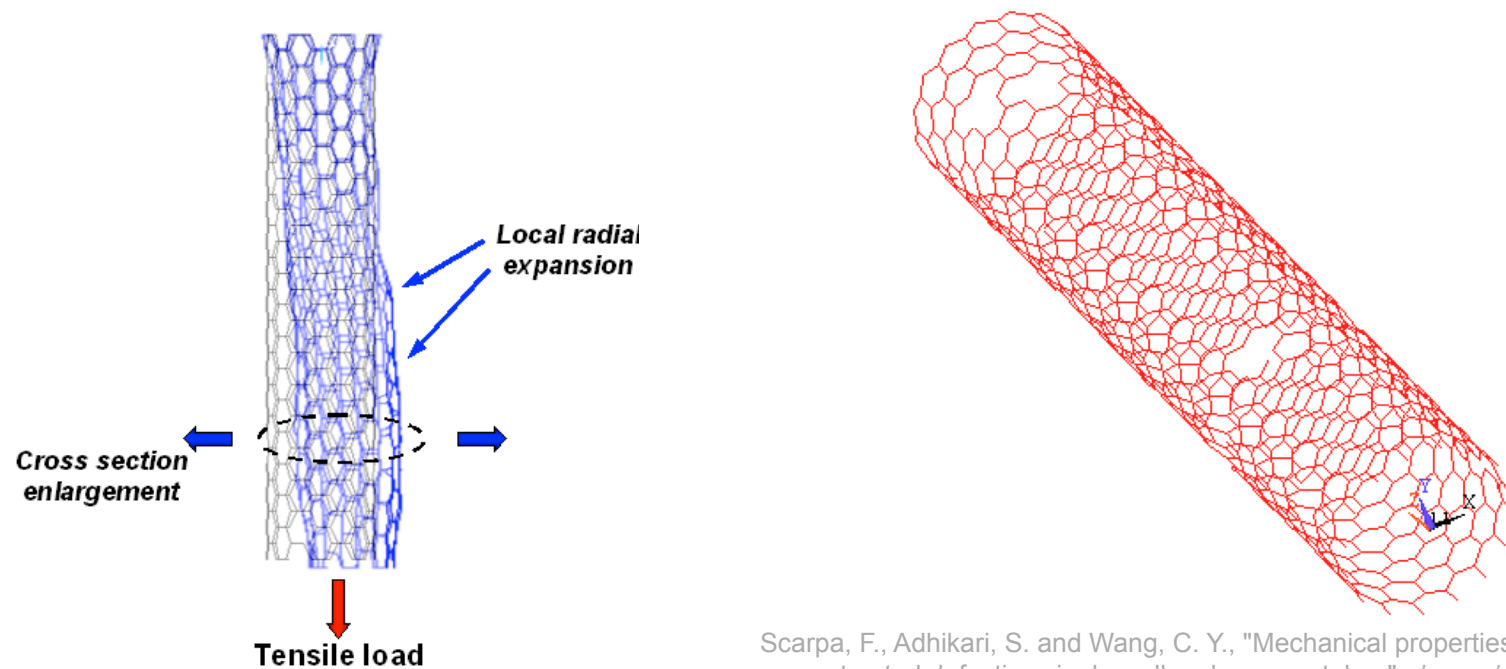


Flores, E. I. S., Adhikari, S., Friswell, M. I. and Scarpa, F., "Hyperelastic axial buckling of single wall carbon nanotubes", Physica E: Low-dimensional Systems and Nanostructures, 44[2] (2011), pp. 525-529.



Carbon nanotubes with defects

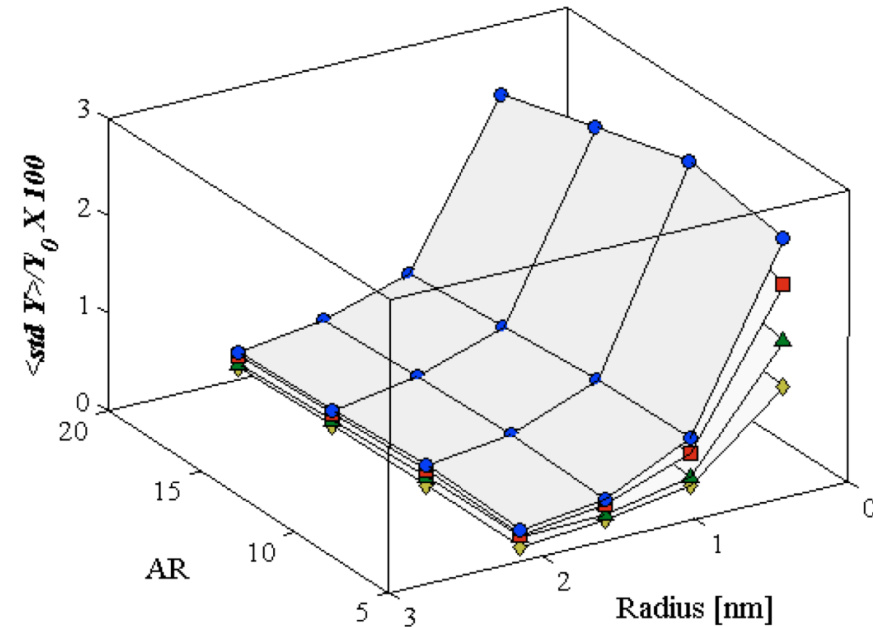
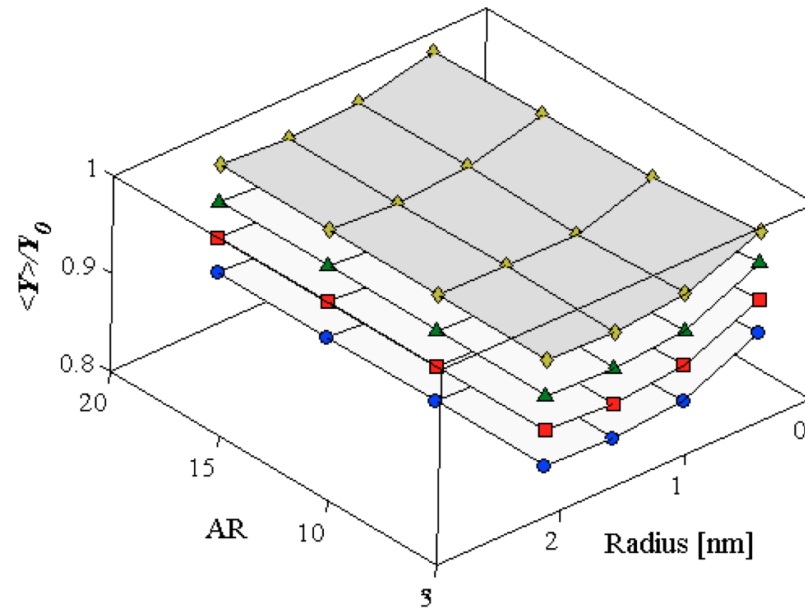
- ◆ We are interested in the changes in the mechanical properties



Scarpa, F., Adhikari, S. and Wang, C. Y., "Mechanical properties of non reconstructed defective single wall carbon nanotubes", *Journal of Physics D: Applied Physics*, 42 (2009) 142002



Carbon nanotubes with defects



(a) Ratio between mean of axial Young's modulus and pristine stiffness and (b) between standard deviation of the Young's modulus against pristine Young's modulus for armchair (n,n). Pristine Young's modulus Y_0 : 2.9, 1.36, 0.91, 0.67 TPa for a thickness $d = 0.084$ nm. ● = 2 % NRV; ■ = 1.5 % NRV; ▲ = 1 % NRV; ◆ = 0.5 % NRV



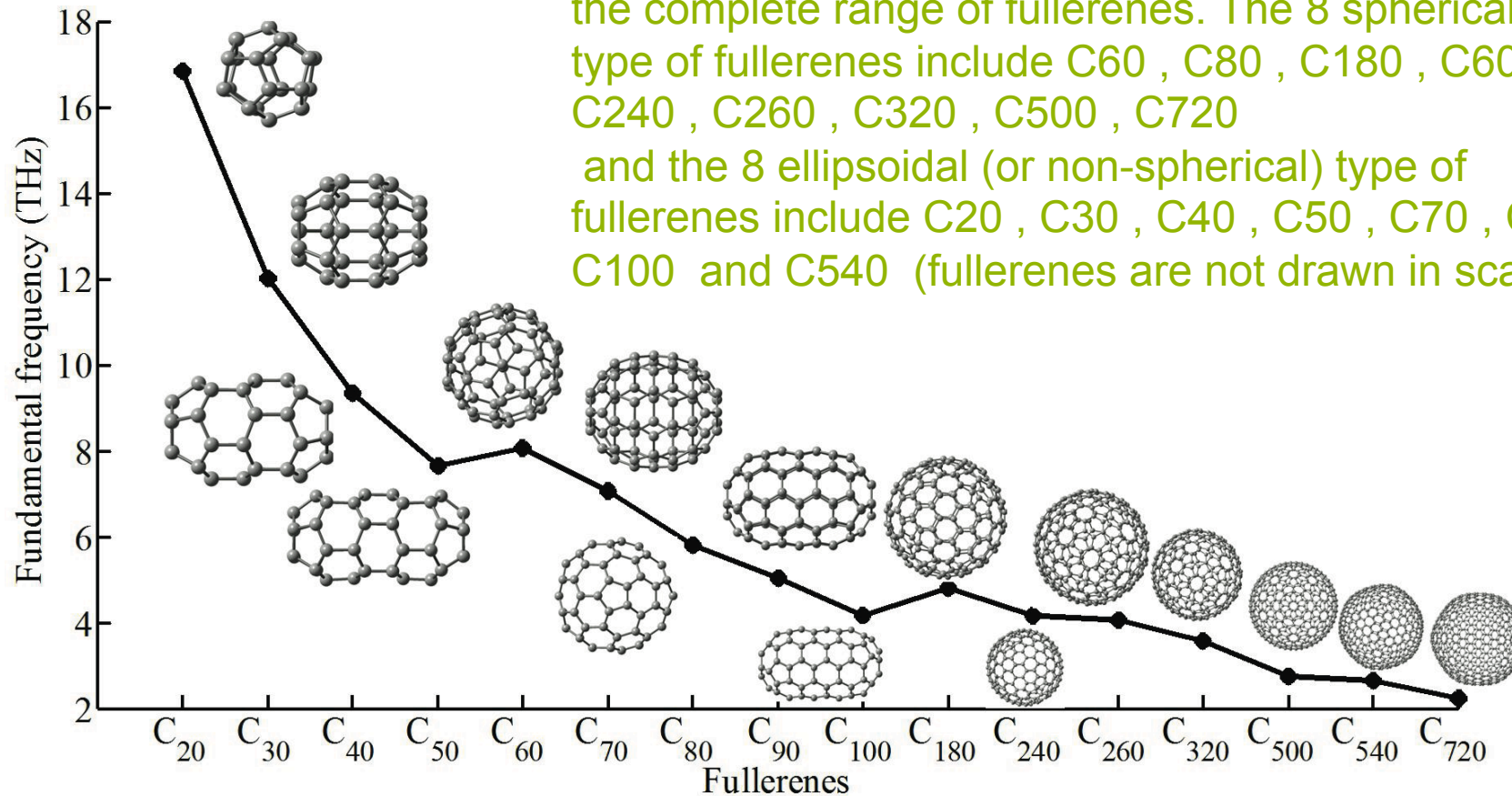
Swansea University
Prifysgol Abertawe

Fullerene



Vibration spectra of fullerene family

The variation of the first natural frequency across the the complete range of fullerenes. The 8 spherical type of fullerenes include C₆₀ , C₈₀ , C₁₈₀ , C₂₄₀ , C₂₆₀ , C₃₂₀ , C₅₀₀ , C₇₂₀ and the 8 ellipsoidal (or non-spherical) type of fullerenes include C₂₀ , C₃₀ , C₄₀ , C₅₀ , C₇₀ , C₉₀ , C₁₀₀ and C₅₄₀ (fullerenes are not drawn in scale).



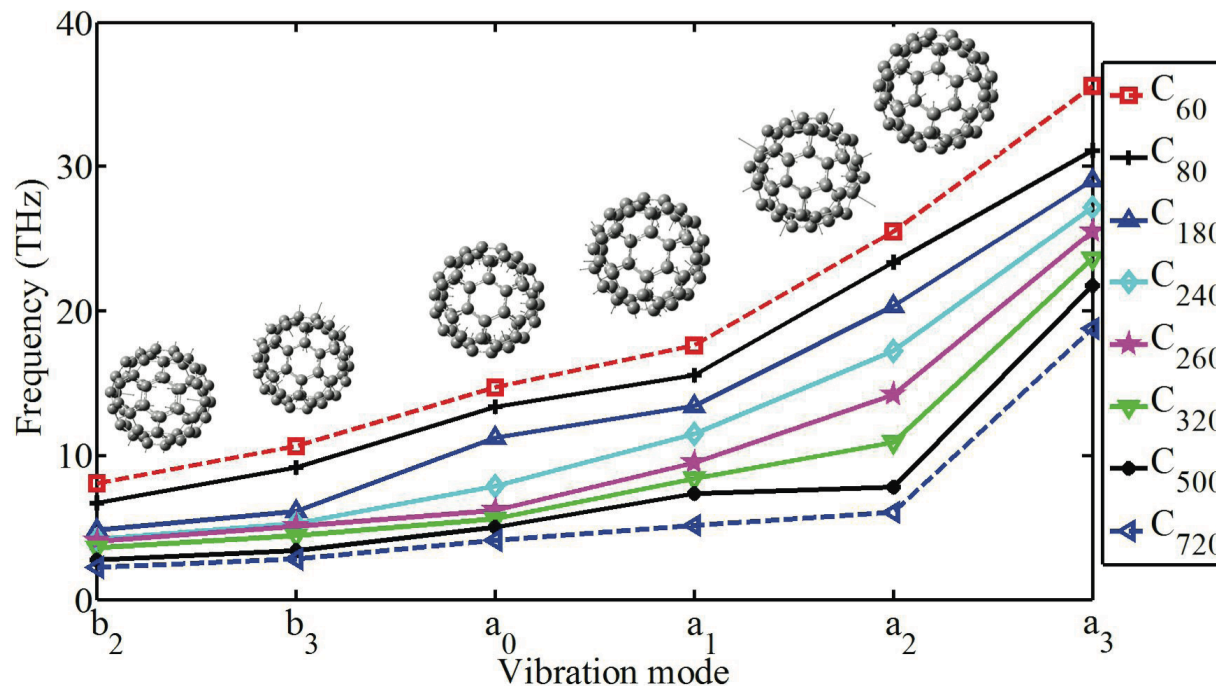
Adhikari, S. and Chowdhury, R., "Vibration spectra of fullerene family", Physics Letters A, 375[22] (2011), pp. 1276-1280.



Thin shell theory

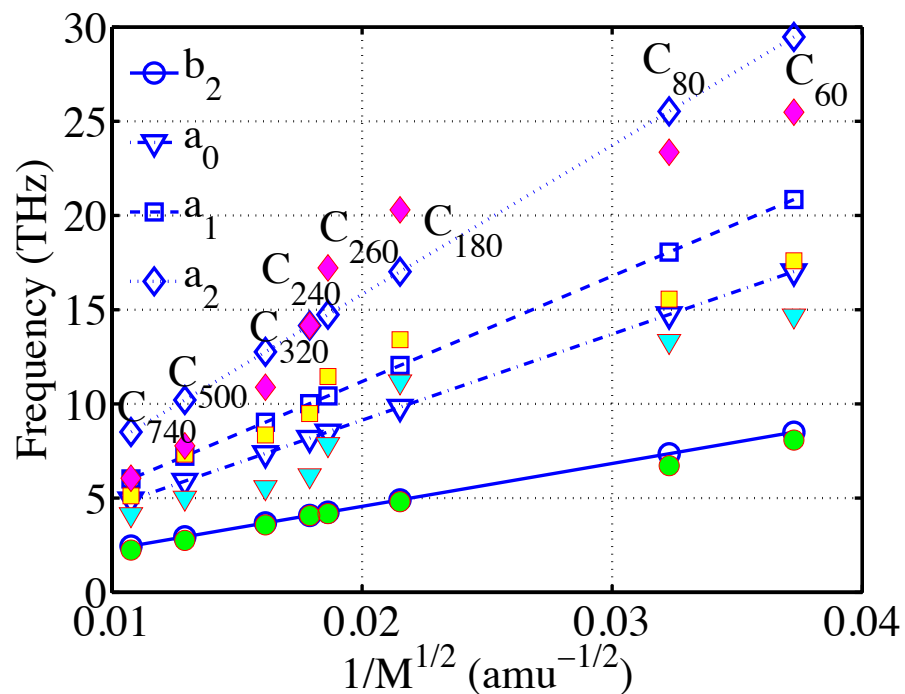
The natural frequencies of spherical fullerenes can be given by

$$\omega_{n1,2}^2 = \frac{E}{R^2 \rho} \Omega_{n1,2}^2 \quad \Omega_{n1,2}^2 = \frac{1}{2(1-\mu^2)} \{n(n+1) + 1 + 3\mu \pm \sqrt{[n(n+1) + 1 + 3\mu]^2 - 4(1-\mu^2)[n(n+1) - 2]}\}$$

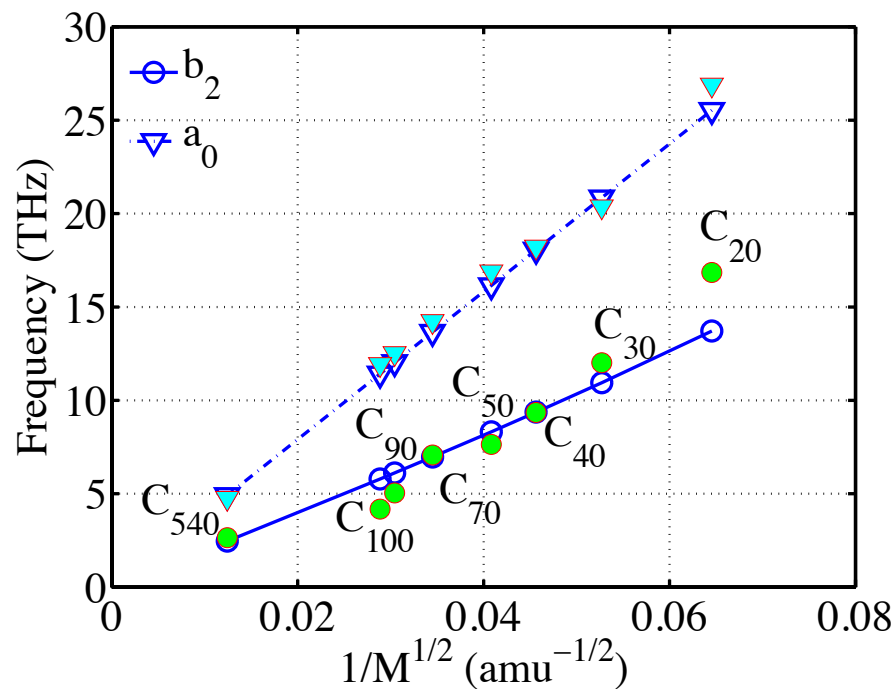




Atomistic Simulation vs Shell theory



Spherical type fullerenes



Ellipsoidal type fullerenes





Swansea University
Prifysgol Abertawe

Graphene



Atomistic FE – in-plane SLGS

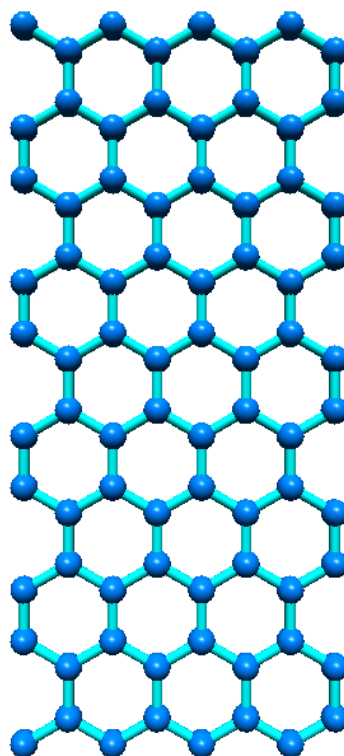


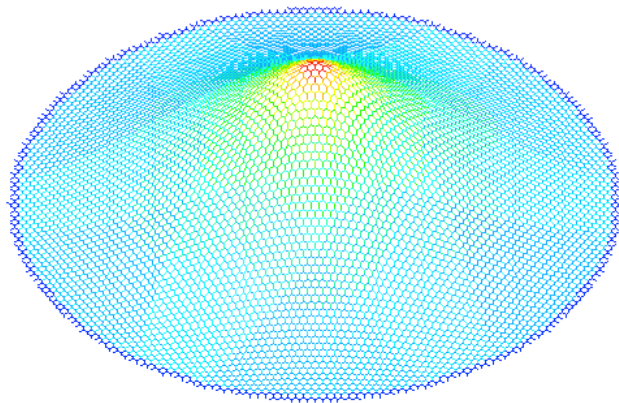
Table 5. Graphene data from literature and present work.

Author	Y_1 (TPa nm)	Y_2 (TPa nm)	ν_{12}	ν_{21}	d (Å)
Tu and Ou-Yang [45]		0.348		0.34	0.74
Zhou <i>et al</i> [46]		0.377		0.24	0.74
Yakobson <i>et al</i> [47]		0.363		0.19	0.66
Caillerie <i>et al</i> [25]		0.277		0.26	N/A
Brenner <i>et al</i> [15]		0.235		0.41	0.62
Huang <i>et al</i> [17]		0.243		0.397	0.57
Kudin <i>et al</i> [13]		0.345		0.149	0.84
Chang and Gao [50]		0.360		0.16	3.4
Cho <i>et al</i> [48]		0.386		0.195	3.35
Sakhae-Pour [34]		0.337–0.354		1.129–1.441	3.4
Hemmasizadeh <i>et al</i> [24]		0.124		0.19	1.317
Blakslee <i>et al</i> [58]		0.342		0.16	3.35
Lee <i>et al</i> [60]		0.335		N/A	3.35
Reddy <i>et al</i> [23]	0.228	0.277	0.43	0.52	3.4
Present FE honeycomb (AMBER)	0.517	0.342	0.523	0.509	0.82–0.99
Present FE honeycomb (Morse)	0.546	0.408	0.551	0.577	0.86–0.87
Present EHM		0.297		0.211	0.84
stretching–hinging (AMBER)					
Present EHM		0.384		0.213	0.74
stretching–hinging (Morse)					
Present EHM		0.144		0.617	0.84
stretching–hinging–shear (AMBER)					
Present EHM		0.169		0.653	0.74
stretching–hinging–shear (Morse)					
Present EHM-all deformation mechanisms (AMBER)		0.064		0.830	0.84
Present EHM-all deformation mechanisms (Morse)		0.074		0.848	0.74

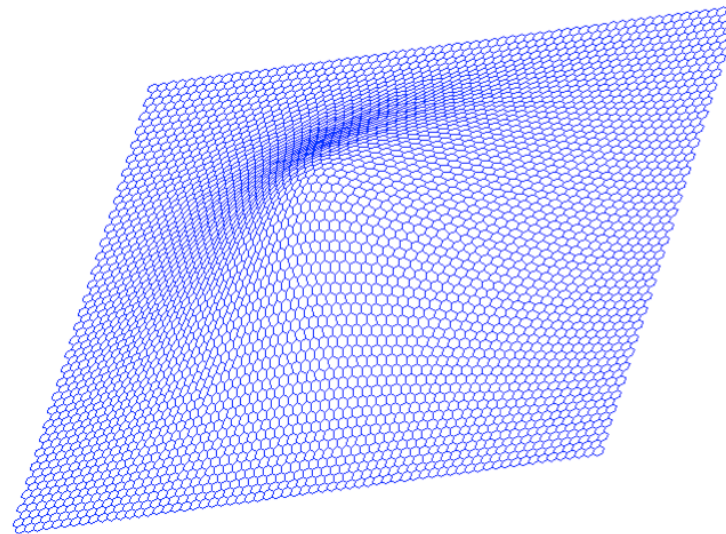
(F Scarpa, S Adhikari, A S Phani, 2009. *Nanotechnology* 20, 065709)



Atomistic FE vs Continuum – SLGS



Circular SLGS ($R = 9.5 \text{ nm}$)
under central loading. Distribution
of equivalent membrane stresses.

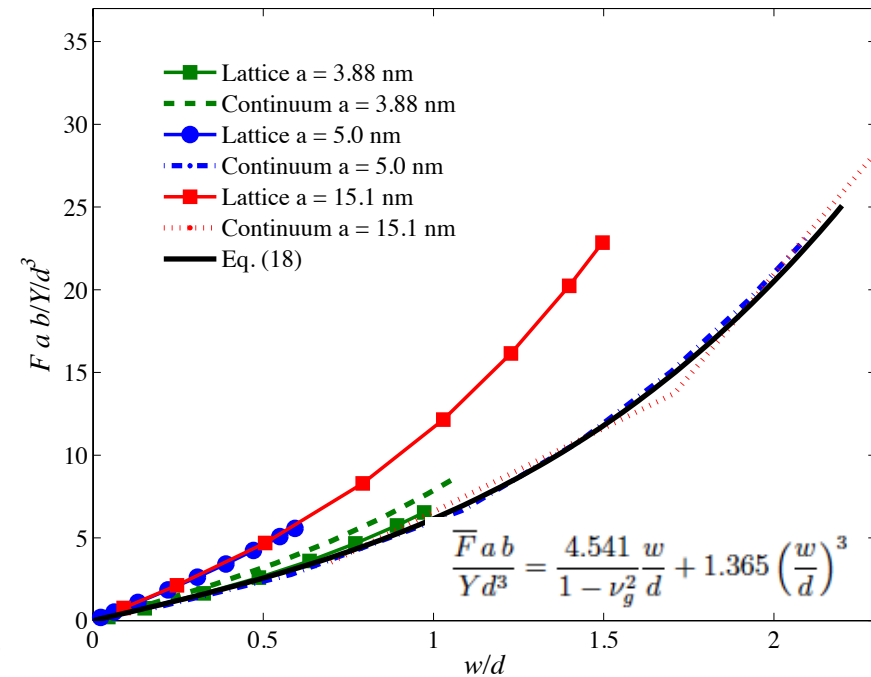
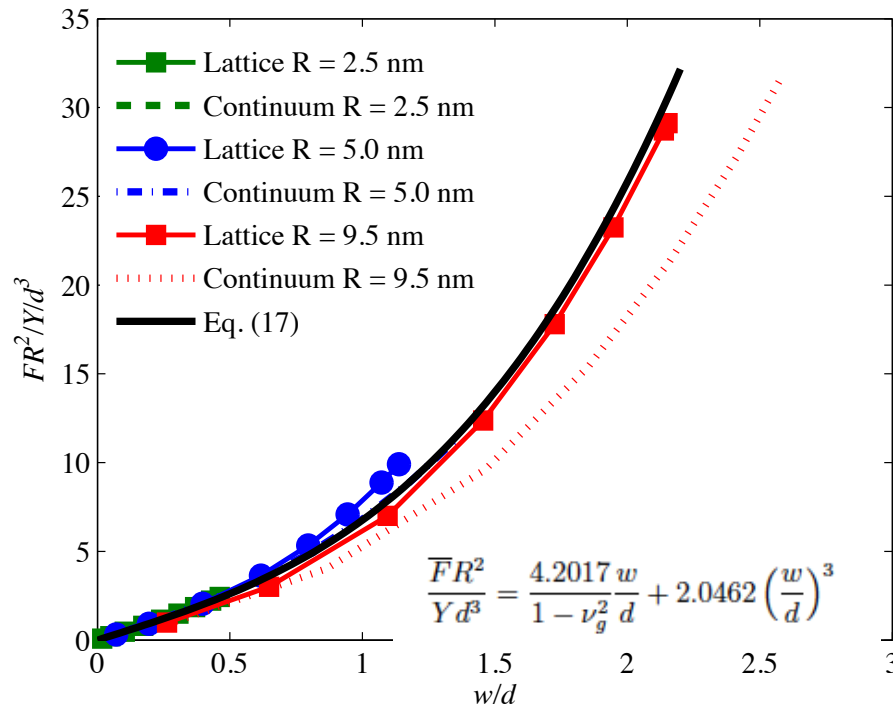


Deformation of rectangular SLGS
($15.1 \times 13.03 \text{ nm}^2$) under central
loading.

Scarpa, F., Adhikari, S., Gil, A. J. and Remillat, C., "The bending of single layer graphene sheets: Lattice versus continuum approach", *Nanotechnology*, 21[12] (2010), pp. 125702:1-9.



Axtomistic FE vs Continuum – SLGS



Comparison of the nondimensional force vs. nondimensional out-of-plane displacement for circular and rectangular lattice and continuum SLGS.





Analytical approach for SLGS – honeycomb structure

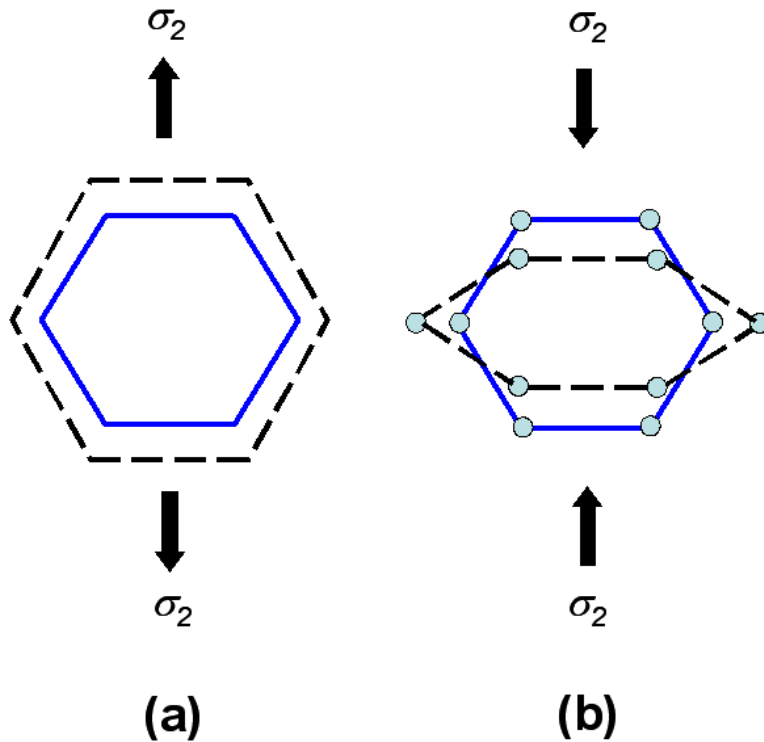
C-C bonds deform under stretching and hinging

$$K_h = \frac{8k_\tau}{d^2} \quad \text{Hinging constant related to thickness } d$$

Applying averaging of stretching and hinging deformation over unit cell:

$$E_1 = \frac{4\sqrt{3}k_r K_h}{3d(k_r + 3K_h)} \quad E_2 = \frac{4\sqrt{3}k_r K_h}{3d(k_r + 3K_h)}$$

$$\nu_{21} = \nu_{12} = \frac{1 - K_h/k_r}{1 + 3K_h/k_r} \quad G_{12} = \frac{\sqrt{3}K_h k_r}{3d(k_r + K_h)}$$

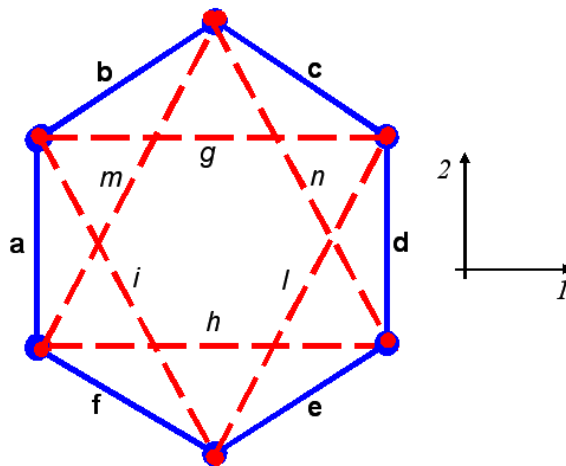


- Isotropic for “infinite” graphene sheet
- Orthotropic for finite size graphene and considering edge effects

F Scarpa, S Adhikari, A S Phani, 2009. *Nanotechnology* 20, 065709



Analytical approach for SLGS – honeycomb structure



Unit cell made by rods withstanding axial and bending deformation

$$Y_{a-f} = \frac{4Lk_r}{\pi d_s^2}$$

Equivalent Young's modulus for axial members

$$Y_{g-n} = \frac{16k_\theta}{\pi L d_b^2}$$

Equivalent Young's modulus for axial members

A **Rigidity** matrix is obtained using a lattice continuum modelling of space frames → equivalence with plane stress formulation for a plane sheet:

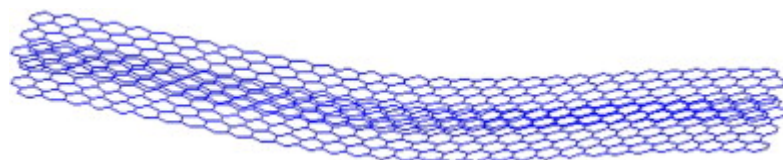
$$E = \frac{1}{d_{\max}} \frac{4\sqrt{3}}{9L^2} (k_r L^2 + 12k_\theta) \quad \nu = \frac{1}{3}$$

F Scarpa, S Adhikari, A S Phani, 2009. *Nanotechnology* **20**, 065709

(L Kollár and I Hegedús. Analysis and design of space frames by the Continuum Method. Developments in Civil Engineering, 10. Elsevier, Amsterdam, 1985)

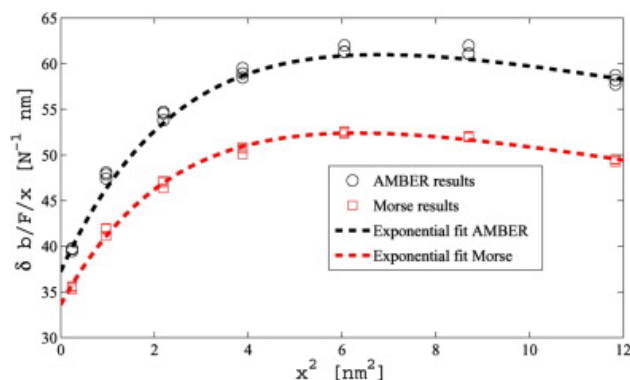
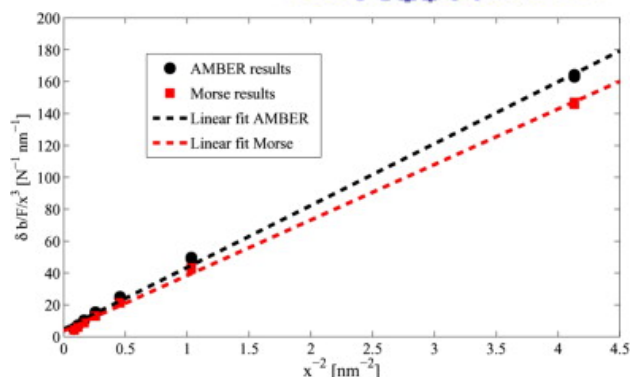


Atomistic FE – Bilayer Graphene



- Equivalent to structural “sandwich” beams
- C-C bonds in graphene layers represented with classical equivalent beam models
- “Core” represented by Lennard-Jones potential interactions:

$$F_{ij} = -12\epsilon \left[\left(\frac{r_{min}}{y} \right)^{13} - \left(\frac{r_{min}}{y} \right)^7 \right] \quad \begin{matrix} r_{min} = 0.383 \text{ nm} \\ \epsilon = 2.39 \text{ meV} \end{matrix}$$



Dimensions [nm × nm]	E_f [TPa]	G_{LJ} [TPa]	Force model
7.99 × 0.92	0.371	0.0142	AMBER
7.99 × 1.35	0.379	0.0143	AMBER
7.99 × 2.63	0.371	0.0143	AMBER
7.99 × 0.92	0.531	0.0161	Morse
7.99 × 1.35	0.535	0.0161	Morse
7.99 × 2.63	0.520	0.0160	Morse

$E_f = 0.5 \text{ TPa}$ (I.W. Frank, D.M. Tanenbaum, A.M. van der Zande, P.L. McEuen, J. Vac. Sci. Technol. B 25 (2007) 2558)

Scarpa, F., Adhikari, S. and Chowdhury, R., "The transverse elasticity of bilayer graphene", Physics Letters A, 374[19-20] (2010), pp. 2053-2057.



Mechanical vibration of SLGS

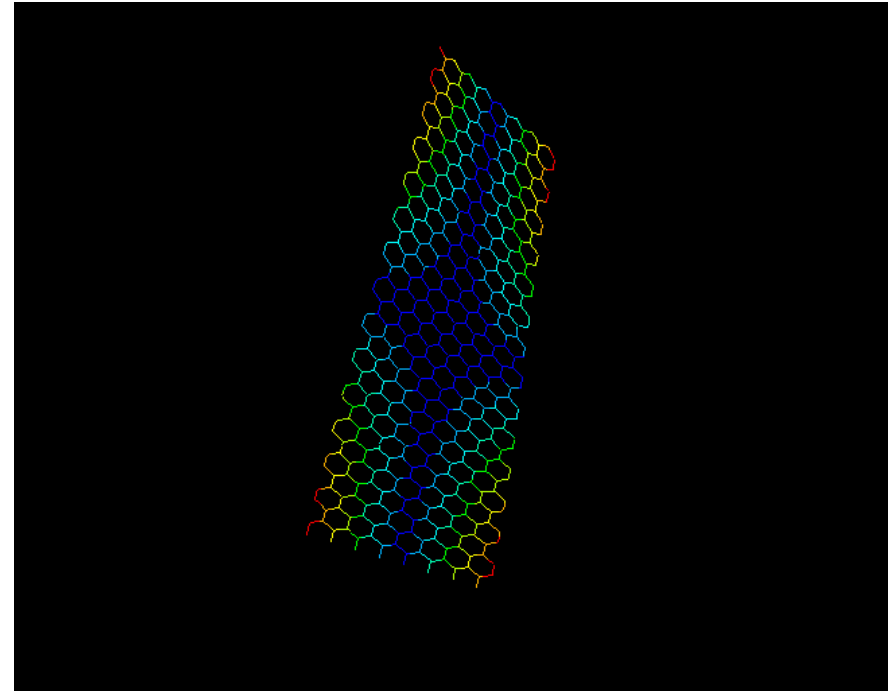
Lumped mass matrix:

$$[\mathbf{M}]_e = \text{diag} \left[\frac{m_c}{3} \quad \frac{m_c}{3} \quad \frac{m_c}{3} \quad 0 \quad 0 \quad 0 \right]$$

Minimisation of the Hamiltonian for the i^{th} mode:

$$H_i = \frac{1}{2} \{\Phi\}_i^T [\mathbf{M}] \{\Phi\}_i \times \omega_i^2 + \frac{1}{2} \{\Phi\}_i^T [\mathbf{K}] \{\Phi\}_i = \omega_i^2$$

Comparison against Molecular Mechanics model based on the eigenvalue analysis of the system Hessian matrix

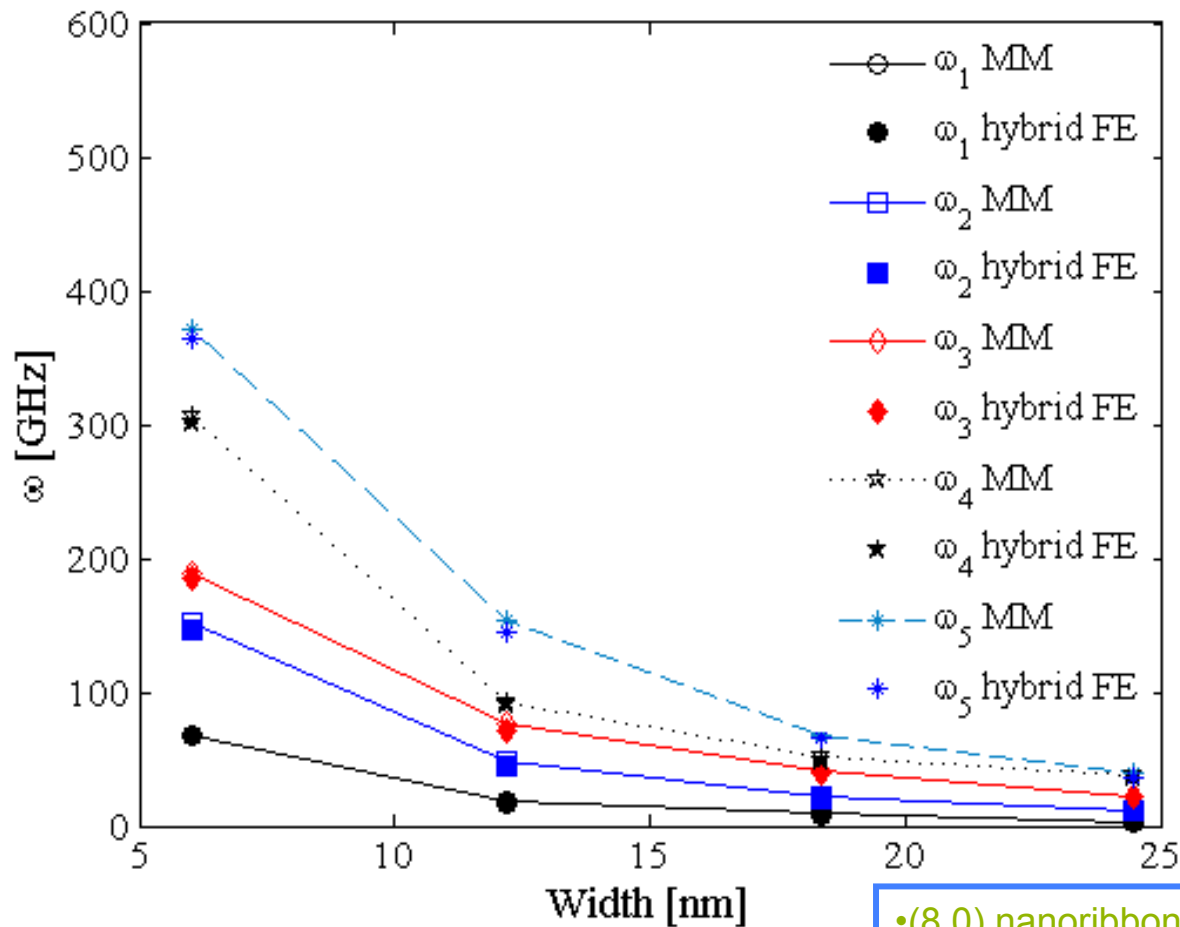


Scarpa, F., Chowdhury, R., Kam, K., Adhikari, S. and Ruzzene, M., "Wave propagation in graphene nanoribbons", *Nanoscale Research Letters*, 6 (2011), pp. 430:1-10.

Chowdhury, R., Adhikari, S., Scarpa, F. and Friswell, M. I., "Transverse vibration of single layer graphene sheets", *Journal of Physics D: Applied Physics*, 44[20] (2011), pp. 205401:1-11.



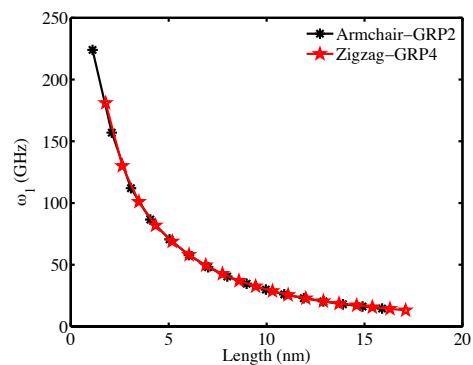
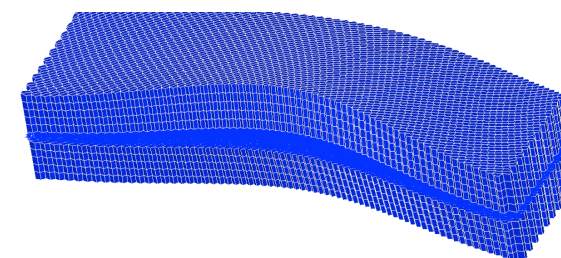
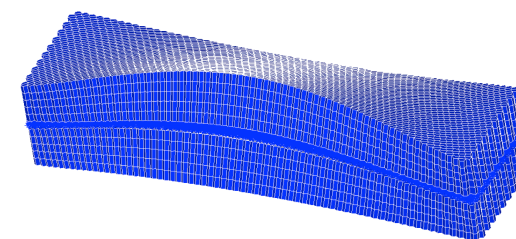
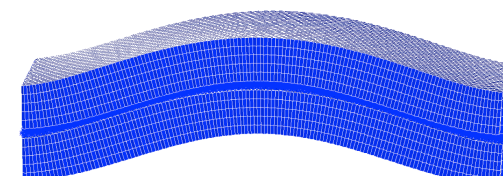
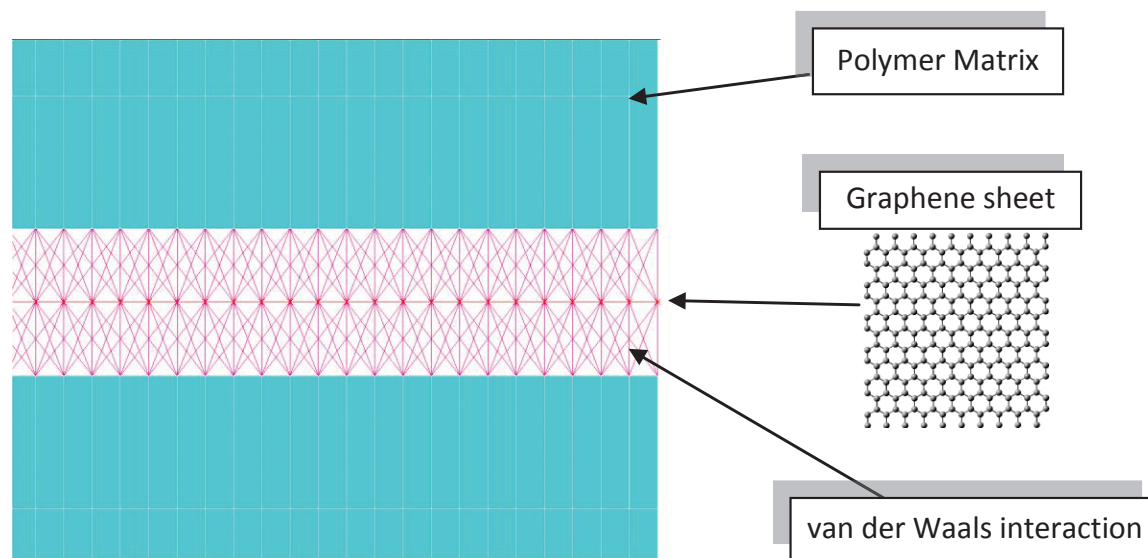
Mechanical vibration of SLGS



- (8,0) nanoribbons with different lengths
- Errors between 2 and 3 %
- Average thickness $d = 0.077$ nm



Graphene composites



Chandra, Y., Chowdhury, R., Scarpa, F., Adhikari, S. and Seinz, J.,
"Multiscale modeling on dynamic behaviour of graphene based
composites", Materials Science and Engineering B, in press.

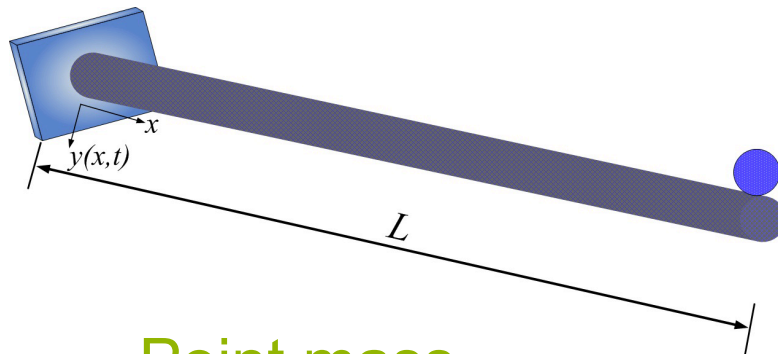
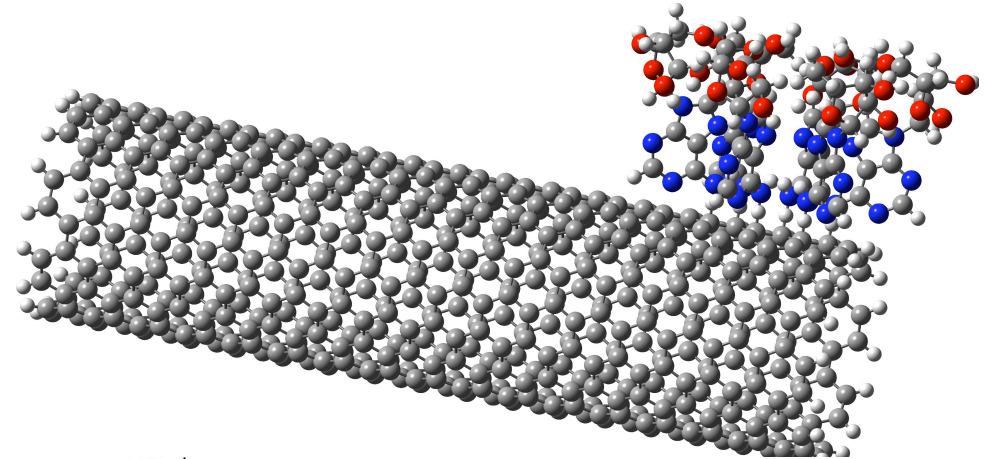
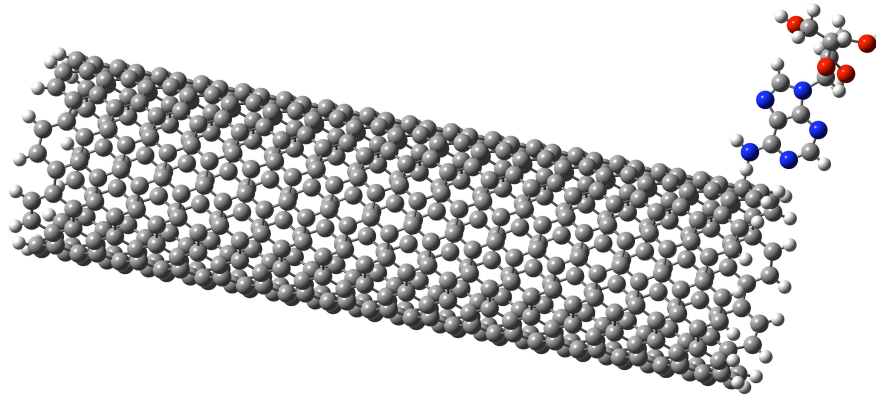


Swansea University
Prifysgol Abertawe

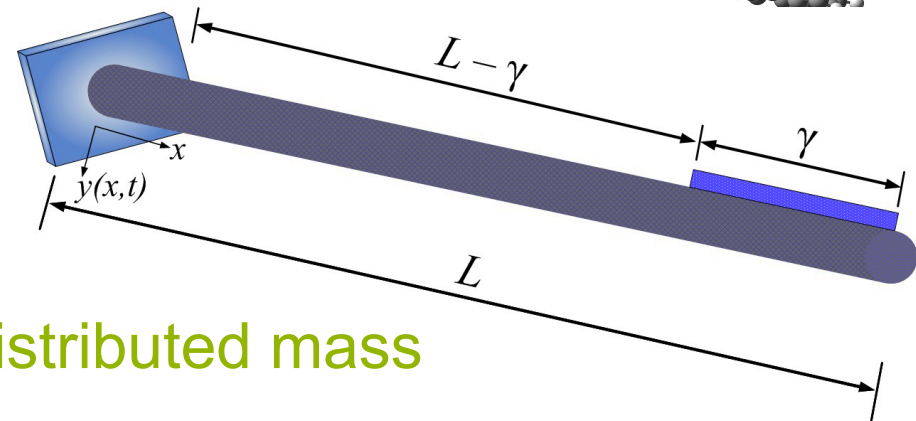
Nanobio Sensors



Vibration based mass sensor: CNT



Point mass



Distributed mass

Chowdhury, R., Adhikari, S. and Mitchell, J., "Vibrating carbon nanotube based bio-sensors", *Physica E: Low-dimensional Systems and Nanostructures*, 42[2] (2009), pp. 104-109.

Adhikari, S. and Chowdhury, R., "The calibration of carbon nanotube based bio-nano sensors", *Journal of Applied Physics*, 107[12] (2010), pp. 124322:1-8



Vibration based mass sensor: CNT

The equation of motion of free-vibration: $EI \frac{\partial^4 y(x, t)}{\partial x^4} + \rho A \frac{\partial^2 y(x, t)}{\partial t^2} = 0$

The resonance frequencies: $f_j = \frac{\lambda_j^2}{2\pi} \sqrt{\frac{EI}{\rho AL^4}} \quad \cos \lambda \cosh \lambda + 1 = 0$

The Mode shapes: $Y_j(\xi) = (\cosh \lambda_j \xi - \cos \lambda_j \xi)$
 $- \left(\frac{\sinh \lambda_j - \sin \lambda_j}{\cosh \lambda_j + \cos \lambda_j} \right) (\sinh \lambda_j \xi - \sin \lambda_j \xi)$

where

$$\xi = \frac{x}{L}$$

We use energy principles to obtain the frequency shift due to the added mass.





Vibration based mass sensor: CNT

Natural frequency with the added mass:

$$f_n = \frac{1}{2\pi} \sqrt{\frac{k_{eq}}{m_{eq}}} = \frac{\beta}{2\pi} \frac{c_k}{\sqrt{1 + c_m \Delta M}}$$

where

$$\beta = \sqrt{\frac{EI}{\rho AL^4}}$$

the stiffness calibration constant

$$c_k = \sqrt{\frac{I_3}{I_1}}$$

and the mass calibration constant

$$c_m = \frac{I_2}{I_1}$$

Identification of the added mass

$$f_n = \frac{f_{0n}}{\sqrt{1 + c_m \Delta M}} \quad (22)$$

The frequency-shift can be expressed using Eq. (22) as

$$\Delta f = f_{0n} - f_n = f_{0n} - \frac{f_{0n}}{\sqrt{1 + c_m \Delta M}} \quad (23)$$

From this we obtain

$$\frac{\Delta f}{f_{0n}} = 1 - \frac{1}{\sqrt{1 + c_m \Delta M}} \quad (24)$$

Rearranging gives the expression

$$\Delta M = \frac{1}{c_m \left(1 - \frac{\Delta f}{f_{0n}}\right)^2} - \frac{1}{c_m} \quad (25)$$



Vibration based mass sensor: CNT

Mass of a nano object can be detected from the **frequency shift** Δf

$$M = \frac{\rho AL}{c_m} \frac{(c_k^2 \beta^2)}{(c_k \beta - 2\pi \Delta f)^2} - \frac{\rho AL}{c_m}$$

$$I_1 = \int_0^1 Y_j^2(\xi) d\xi = 1.0$$

$$I_2 = \frac{1}{\gamma} \int_{\xi=1-\gamma}^1 Y_j^2(\xi) d\xi; \quad 0 \leq \gamma \leq 1$$

$$I_3 = \int_0^1 Y_j''^2(\xi) d\xi = 12.3624$$

$$c_k = \sqrt{\frac{I_3}{I_1}} = 3.5160 \quad \text{and} \quad c_m = \frac{I_2}{I_1}$$

TABLE I. The stiffness (c_k) and mass (c_m) calibration constants for CNT based bio-nano sensor. The value of γ indicates the length of the mass as a fraction of the length of the CNT.

Mass size	Cantilevered CNT		Bridged CNT	
	c_k	c_m	c_k	c_m
Point mass ($\gamma \rightarrow 0$)	3.5160152	4.0	22.373285	2.522208547
$\gamma = 0.1$		3.474732666		2.486573805
$\gamma = 0.2$		3.000820053		2.383894805
$\gamma = 0.3$		2.579653837		2.226110255
$\gamma = 0.4$		2.212267400		2.030797235
$\gamma = 0.5$		1.898480438		1.818142650
$\gamma = 0.6$		1.636330135		1.607531183
$\gamma = 0.7$		1.421839146		1.414412512
$\gamma = 0.8$		1.249156270		1.248100151

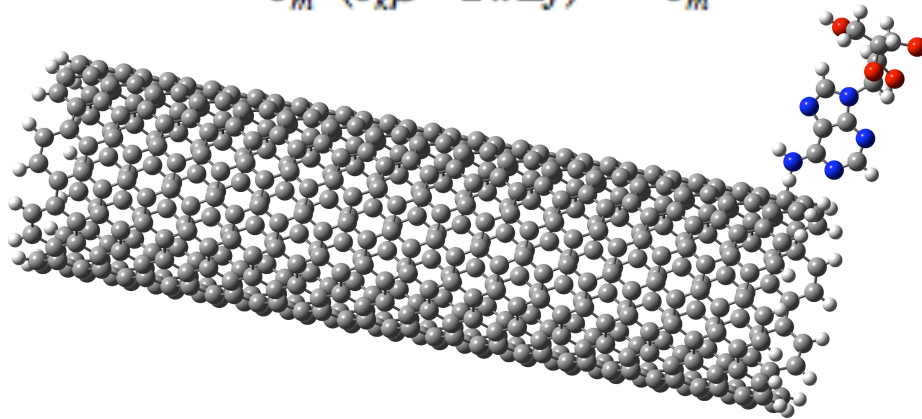
Adhikari, S. and Chowdhury, R., "The calibration of carbon nanotube based bio-nano sensors", *Journal of Applied Physics*, **107**[12] (2010), pp. 124322:1-8



Vibration based mass sensor: CNT

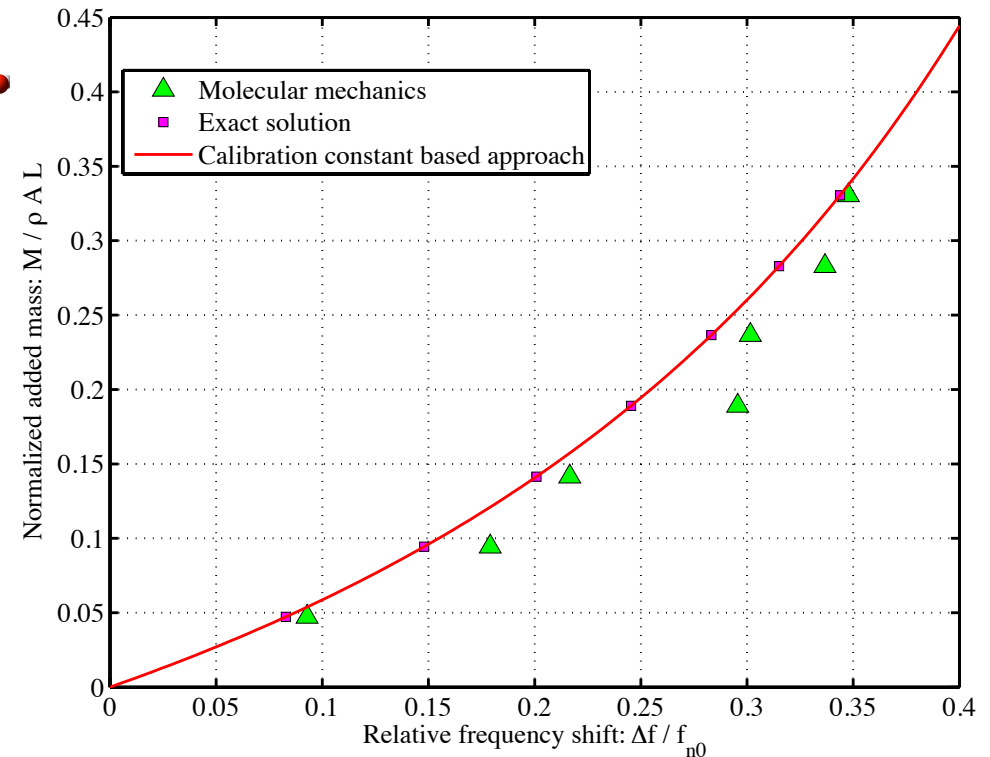
Mass of a nano object can be detected from the frequency shift Δf

$$M = \frac{\rho AL}{c_m} \frac{(c_k^2 \beta^2)}{(c_k \beta - 2\pi \Delta f)^2} - \frac{\rho AL}{c_m}$$



CNT with deoxythymidine

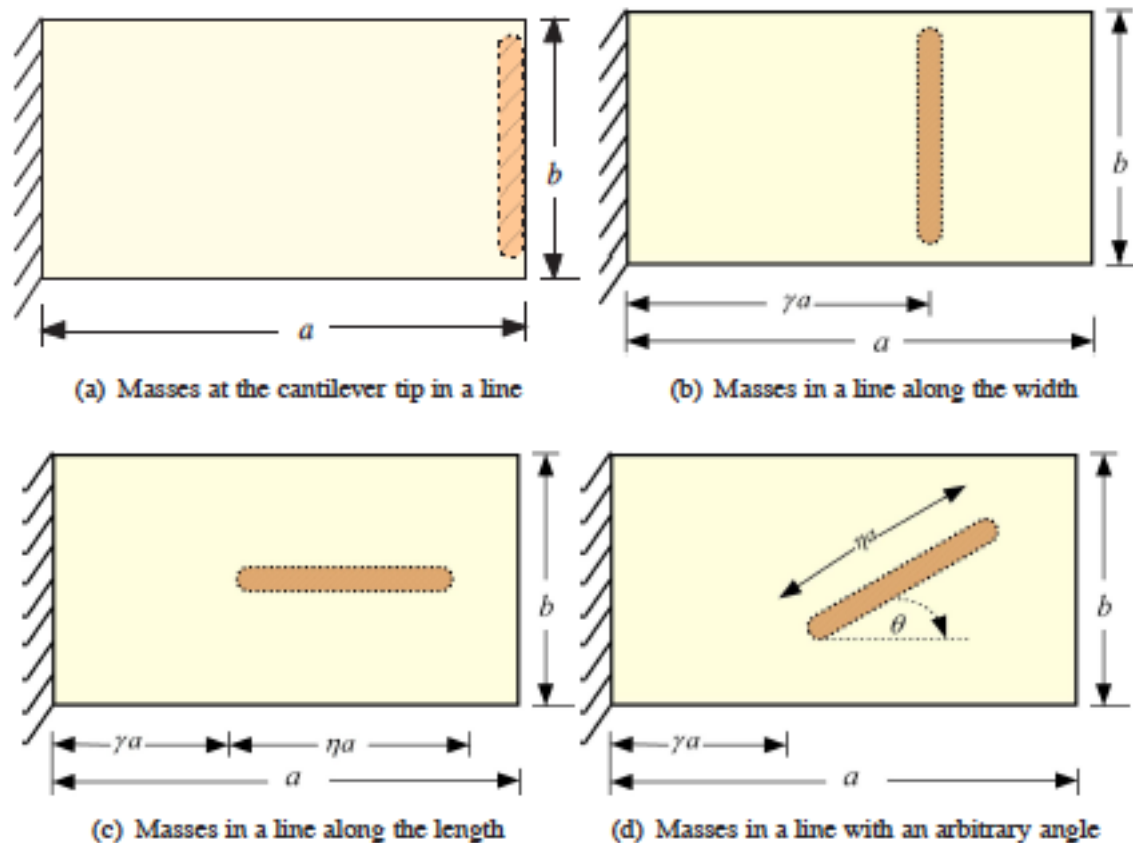
Adhikari, S. and Chowdhury, R., "The calibration of carbon nanotube based bio-nano sensors", *Journal of Applied Physics*, **107**[12] (2010), pp. 124322:1-8





Vibration based mass sensor: Graphene

Vibrating graphene sheets can be used as sensors with different mass arrangements





Vibration based mass sensor: Graphene

Relative added mass:

$$\mu = \frac{1}{c_n \left(1 - \frac{\Delta f}{f_0}\right)^2} - \frac{1}{c_n}$$

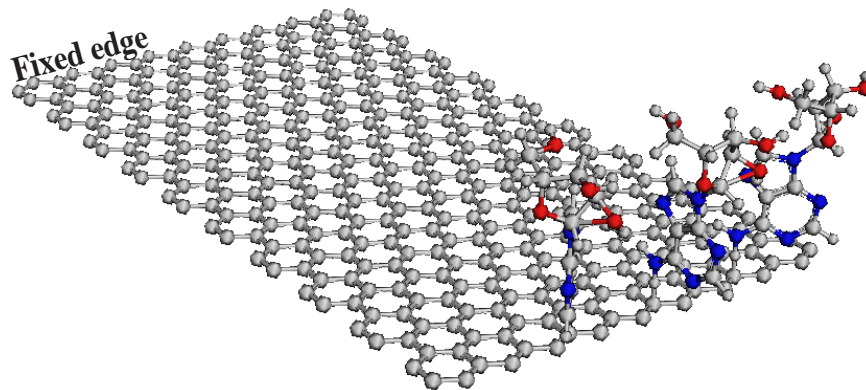
Table 1: The calibration constants for SLGS based bio-nano sensor due to four possible configurations of attached mass.

Mass arrangement	Calibration constant c_n
Case (a): Masses are at the cantilever tip in a line	$2\pi/(3\pi - 8)$
Case (b): Masses are in a line along the width	$2\pi(1 - \cos(\pi\gamma/2))^2/(3\pi - 8)$
Case (c): Masses are in a line along the length	$(3\pi\eta + [\sin((\gamma + \eta)\pi) - \sin(\gamma\pi)] - 8[\sin((\gamma + \eta)\pi/2) - \sin(\gamma\pi/2)])/(\eta(3\pi - 8))$
Case (d): Masses are in a line with an arbitrary angle θ	$(3\pi\eta \cos(\theta) + [\sin((\gamma + \eta \cos(\theta))\pi) - \sin(\gamma\pi)] - 8[\sin((\gamma + \eta \cos(\theta))\pi/2) - \sin(\gamma\pi/2)])/(\eta \cos(\theta)(3\pi - 8))$

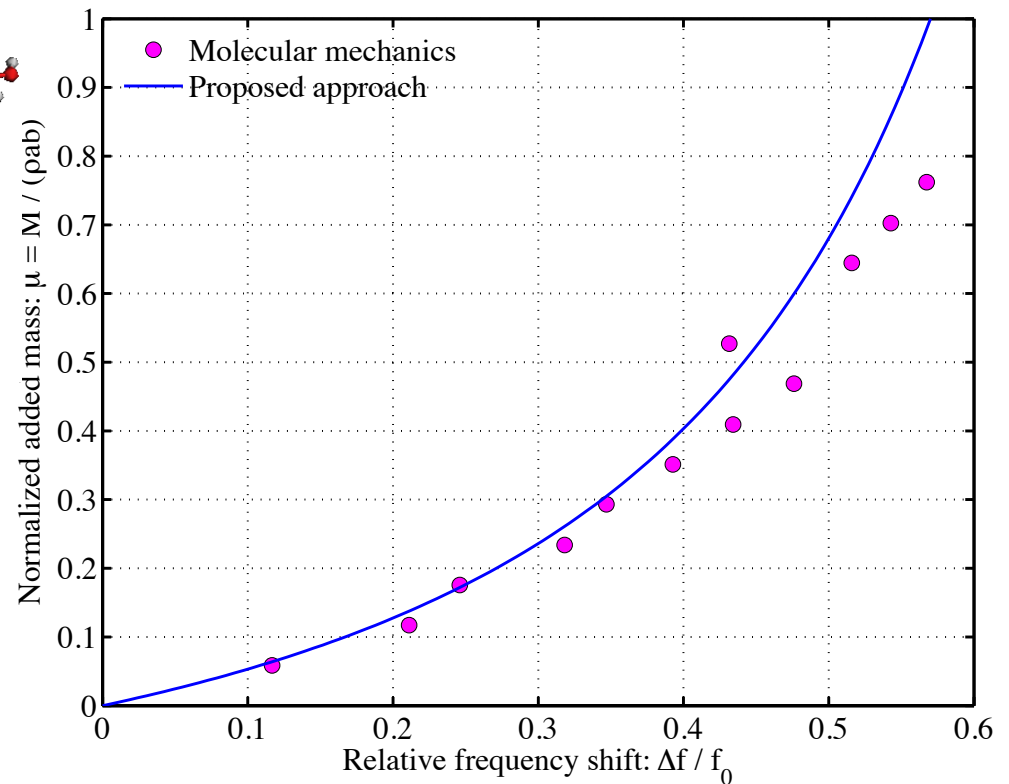


Vibration based mass sensor: Graphene

Vibrating graphene sheets can be used as sensors with different mass arrangements



SLGS with adenosine



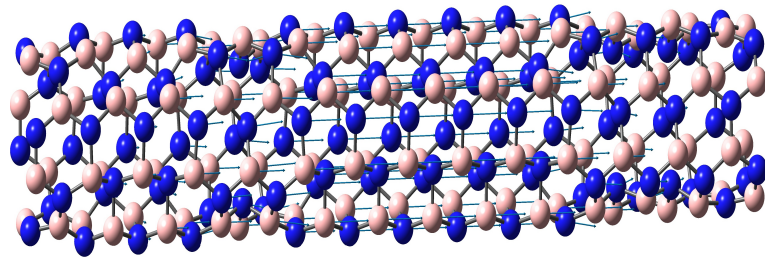


Swansea University
Prifysgol Abertawe

Boron Nitride Nanotube and Nanosheets

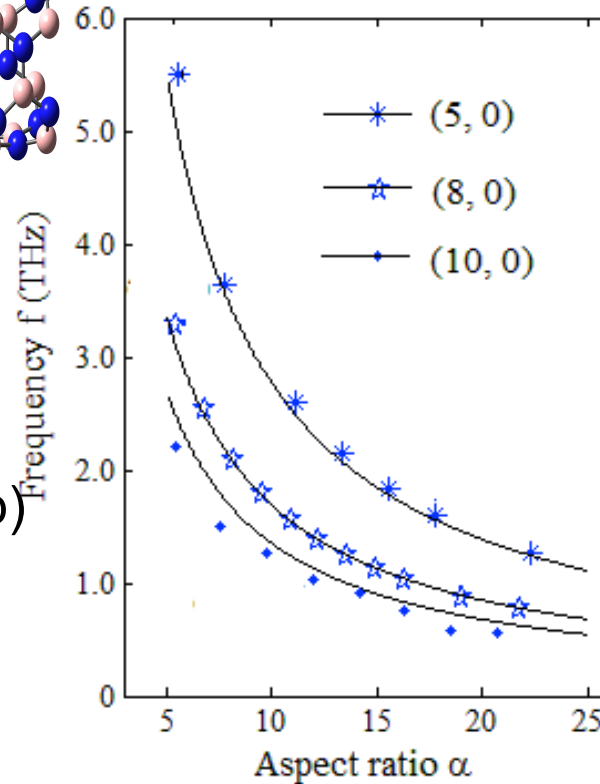


Axial vibration of BNNT

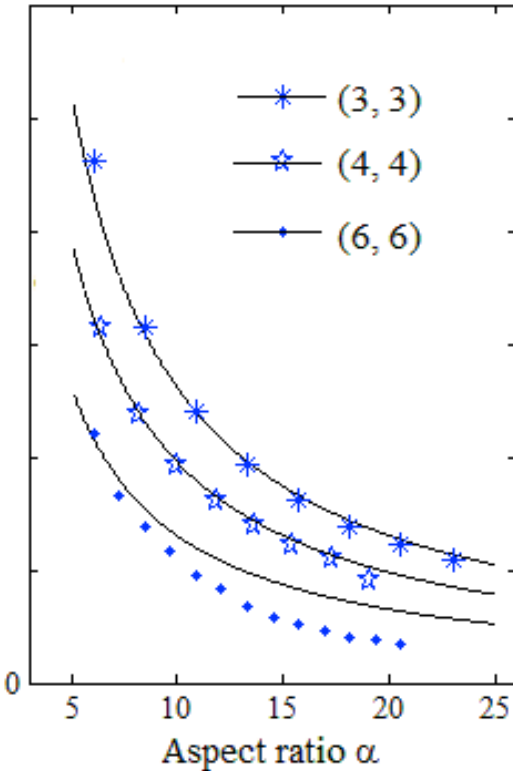


(a)

(a) Axial vibration and its associated frequency of (b) zigzag and (c) armchair BNNTs given by the MM simulations (discrete dots) and a column model with Young's modulus 1TPa (solid lines).



(b)

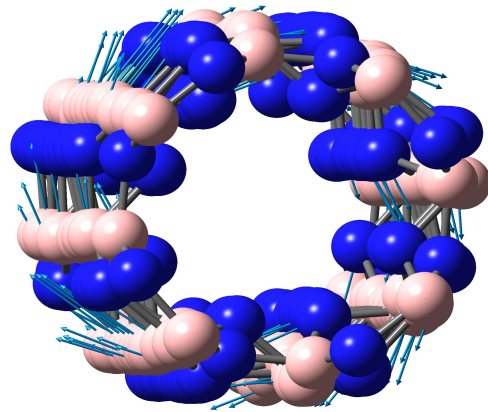


(c)

Chowdhury, R., Wang, C. W., Adhikari, S. and Scarpa, F., "Vibration and symmetry-breaking of boron nitride nanotubes", *Nanotechnology*, 21[36] (2010), pp. 365702:1-9.

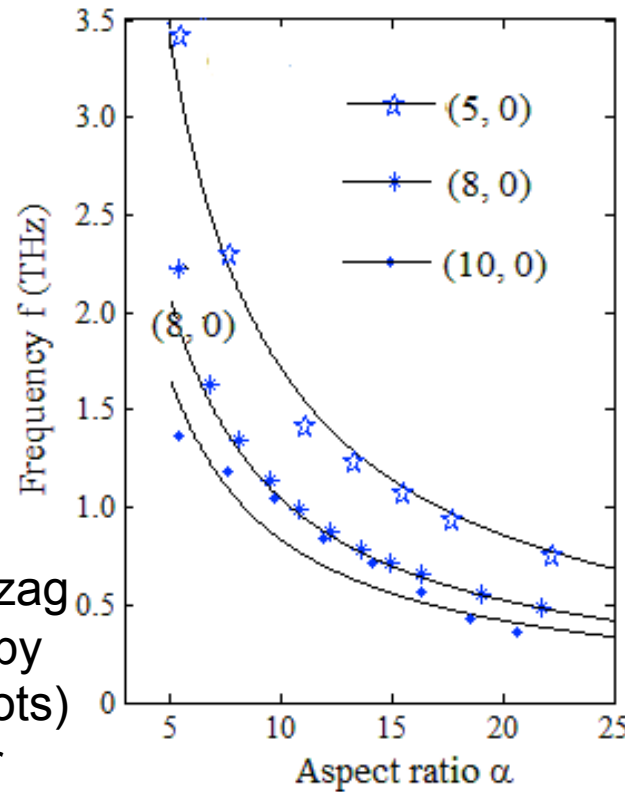


Torsional vibration of BNNT

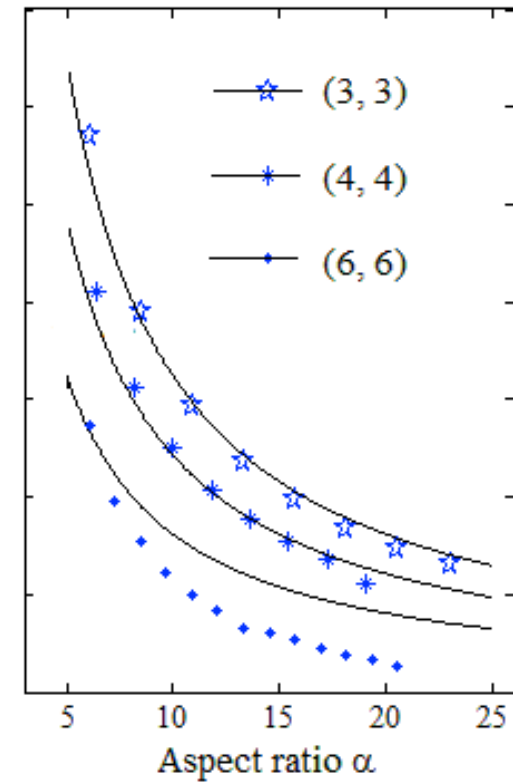


(a)

(a) Torsional vibration and its associated frequency of (b) zigzag and (c) armchair BNNTs given by the MM simulations (discrete dots) and a column model with shear modulus 0.41TPa (solid lines).



(b)

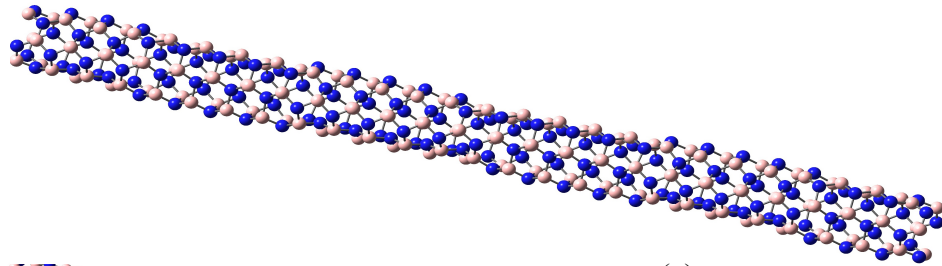


(c)

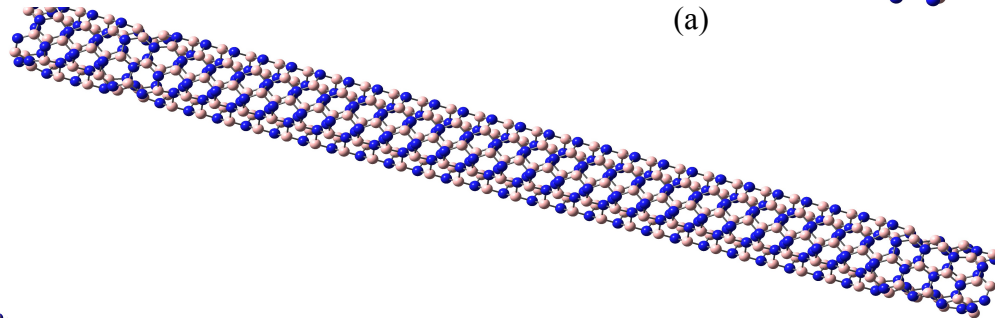
Chowdhury, R., Wang, C. W., Adhikari, S. and Scarpa, F., "Vibration and symmetry-breaking of boron nitride nanotubes", *Nanotechnology*, 21[36] (2010), pp. 365702:1-9.



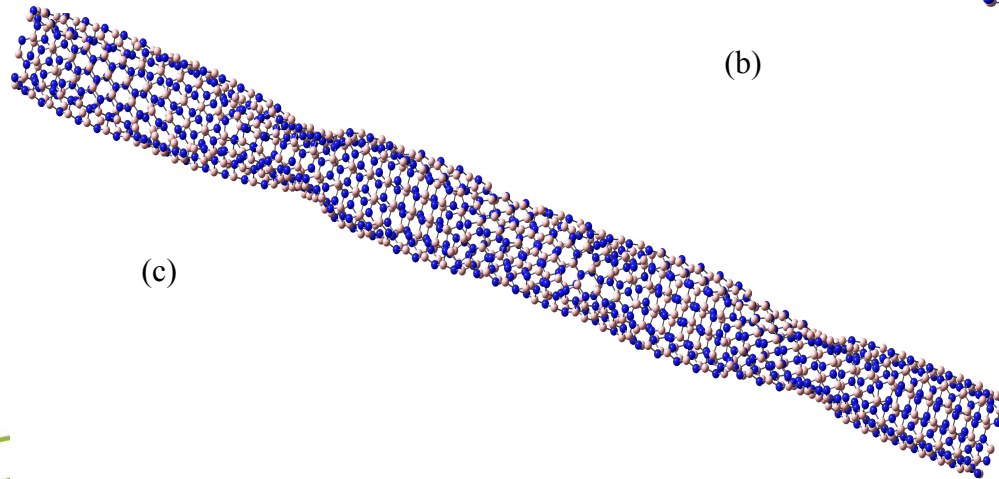
Optimised shape of BNNT



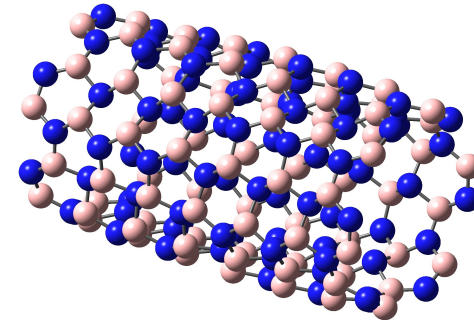
(a)



(b)



(c)

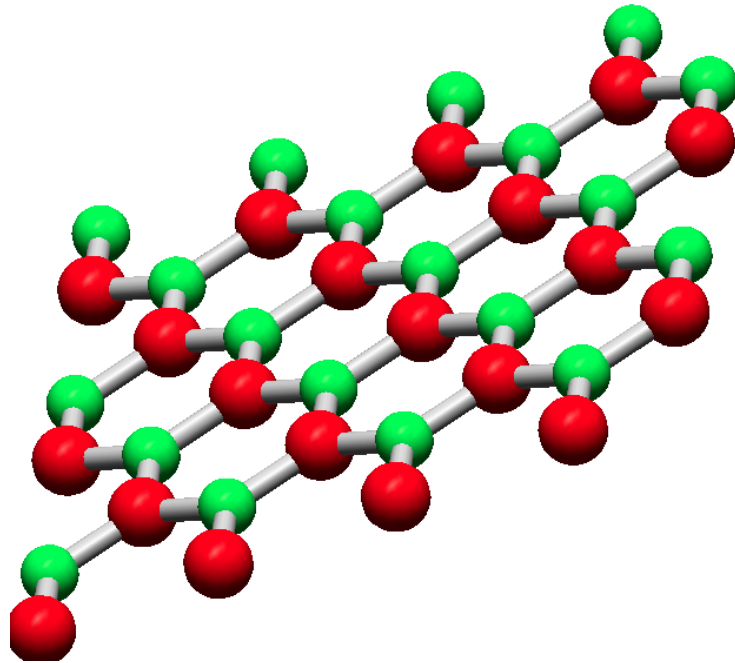


(d)

Optimized configuration of armchair BNNTs: (a) (3, 3), (b) (4,4) and (c) (6,6) with the aspect ratio 15, and (d) short (6, 6) with the aspect ratio 2.



Mechanical property of BN Sheets



Example of armchair (4, 0) BN sheet.
Boron atoms are in red, nitrogen
atoms are in green.

Boldrin, L., Scarpa, F., Chowdhury, R., Adhikari, S. and Ruzzene, M., "Effective mechanical properties of hexagonal boron nitride nanosheets", *Nanotechnology*, 22[50] (2011), pp. 505702:1-7.

$$\bar{Y} = \frac{8\sqrt{3}C_p}{18 + r_{BN}^2 \left(\frac{C_p}{C_\theta}\right)}$$

$$\bar{\nu} = \frac{r_{BN}^2 \left(\frac{C_p}{C_\theta}\right) - 6}{18 + r_{BN}^2 \left(\frac{C_p}{C_\theta}\right)}$$

$$\bar{G} = \frac{2\sqrt{3}C_p}{3 + 18r_{BN}^2 \left(\frac{C_p}{C_\theta}\right)}$$



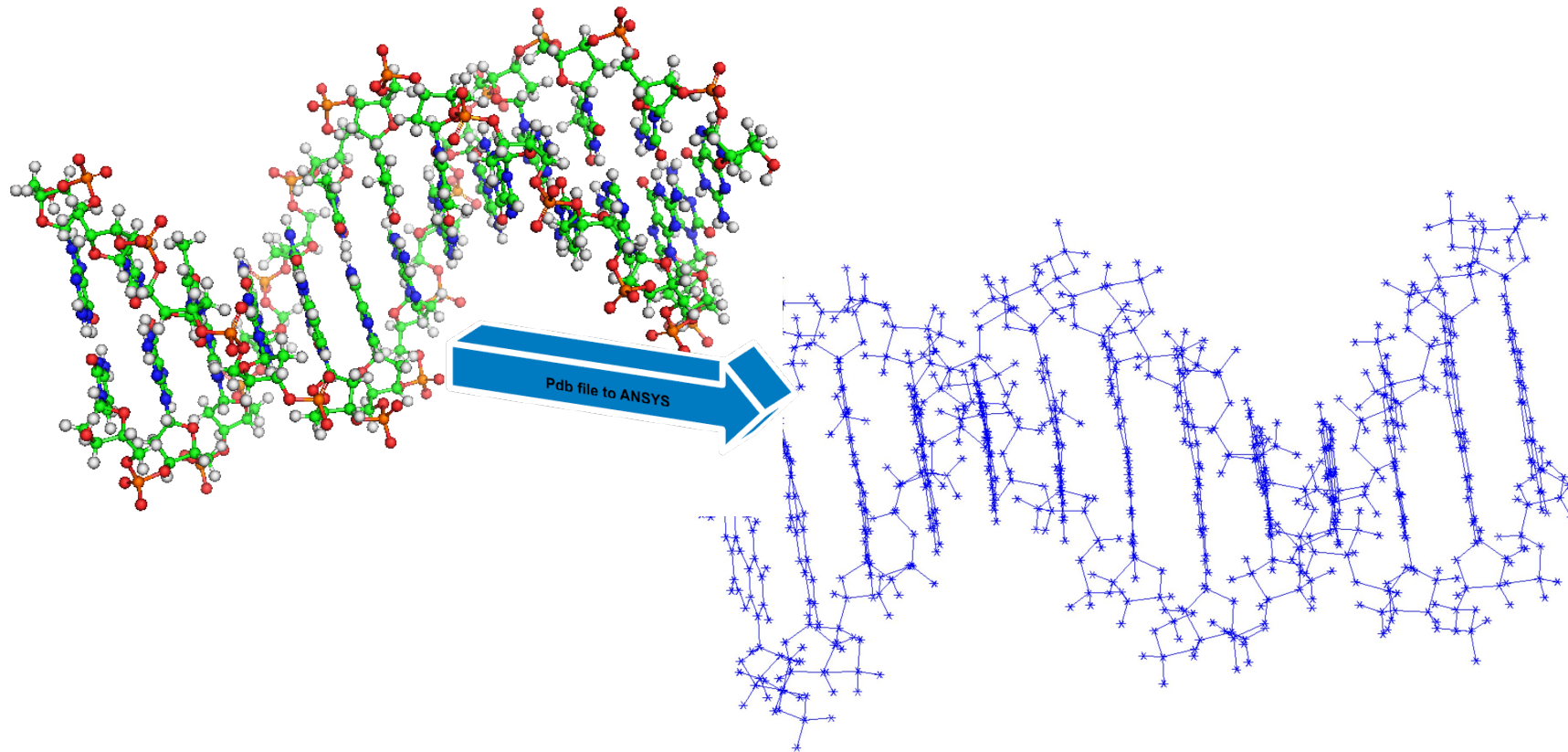
Swansea University
Prifysgol Abertawe

DNA Mechanics



Atomistic FE of DNA

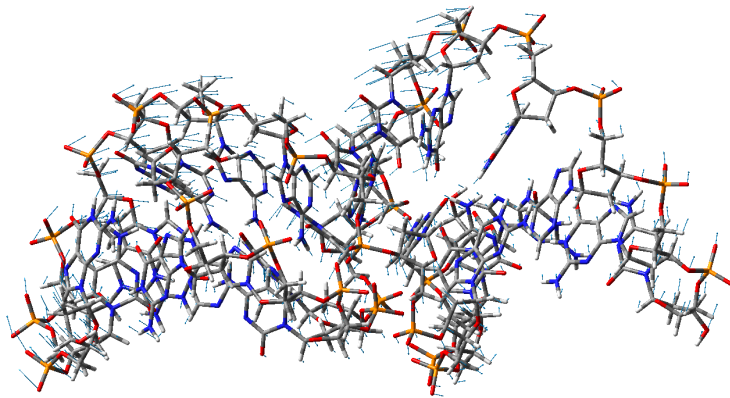
From protein data bank file to ANSYS input file – **a new code for automatic translation**



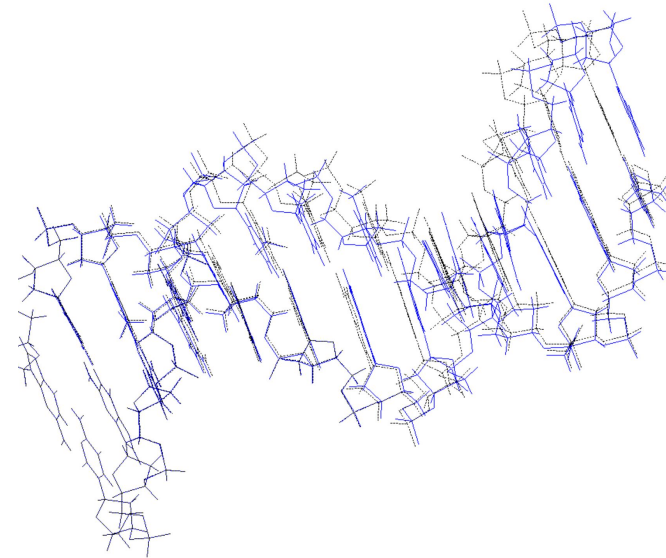


Atomistic FE of DNA

Material properties of the beams are obtained depending on the nature of the bonds



Mode 3 (MM:33.679; FE 38.768 GHz)



Mode 6 (MM:111.696; FE 112.71 GHz)



Conclusions

- Atomistic finite element method is developed for general nanoscale structures:
 - Carbon nanotube
 - Fullerenes
 - Graphene
 - Nanoscale bio sensors
- Programs have been written to convert pdb files to Finite Element geometry file and material properties
- Encouraging results compared to MM simulation were obtained
- Future: nonlinearity, large-scale problems such as proteins & nanocomposites, molecular dynamic simulations, experimental validation



References

1. Murmu, T. and Adhikari, S., "Nonlocal frequency analysis of nanoscale biosensors", *Sensors & Actuators: A. Physical*, 173[1] (2012), pp. 41-48.
2. Boldrin, L., Scarpa, F., Chowdhury, R., Adhikari, S. and Ruzzene, M., "Effective mechanical properties of hexagonal boron nitride nanosheets", *Nanotechnology*, 22[50] (2011), pp. 505702:1-7.
3. Murmu, T., Seinz, J., Adhikari, S. and Arnold, C., "Nonlocal buckling behaviour of bonded double-nanoplate-system", *Journal of Applied Physics*, 110[8] (2011), pp. 084316:1-8.
4. Flores, E. I. S., Adhikari, S., Friswell, M. I. and Scarpa, F., "Hyperelastic axial buckling of single wall carbon nanotubes", *Physica E: Low-dimensional Systems and Nanostructures*, 44[2] (2011), pp. 525-529.
5. Murmu, T. and Adhikari, S., "Nonlocal vibration of bonded double-nanoplate-systems", *Composites Part B: Engineering*, 42[7] (2011), pp. 1901-1911.
6. Chandra, Y., Chowdhury, R., Adhikari, S. and Scarpa, F., "Elastic instability of bilayer graphene using atomistic finite element", *Physica E: Low-dimensional Systems and Nanostructures*, 44[1] (2011), pp. 12-16.
7. Scarpa, F., Chowdhury, R., Kam, K., Adhikari, S. and Ruzzene, M., "Wave propagation in graphene nanoribbons", *Nanoscale Research Letters*, 6 (2011), pp. 430:1-10.
8. Chowdhury, R. and Adhikari, S., "Boron nitride nanotubes as zeptogram-scale bio-nano sensors: Theoretical investigations", *IEEE Transactions on Nanotechnology*, 10[4] (2011), pp. 659-667.
9. Chandra, Y., Chowdhury, R., Scarpa, F. and Adhikari, S., "Vibrational characteristics of bilayer graphene sheets", *Thin Solid Films*, 519[18] (2011), pp. 6026-6032.
10. Adhikari, S. and Chowdhury, R., "Vibration spectra of fullerene family", *Physics Letters A*, 375[22] (2011), pp. 1276-1280.



References

11. Murmu, T., Adhikari, S. and Wang, C. W., "Torsional vibration of carbon nanotube-buckyball systems based on nonlocal elasticity theory", *Physica E: Low-dimensional Systems and Nanostructures*, 43[6] (2011), pp. 1276-1280.
12. Wang, C. W. and Adhikari, S., "ZnO-CNT composite nanowires as nanoresonators", *Physics Letters A*, 375[22] (2011), pp. 2171-2175.
13. Chowdhury, R., Adhikari, S., Scarpa, F. and Friswell, M. I., "Transverse vibration of single layer graphene sheets", *Journal of Physics D: Applied Physics*, 44[20] (2011), pp. 205401:1-11.
14. Scarpa, F., Chowdhury, R., and Adhikari, S., "Thickness and in-plane elasticity of Graphane", *Physics Letters A*, 375[20] (2011), pp. 2071-2074.
15. Wang, C. W., Murmu, T. and Adhikari, S., "Mechanisms of nonlocal effect on the vibration of nanoplates", *Applied Physics Letters*, 98[15] (2011), pp. 153101:1-3.
16. Murmu, T. and Adhikari, S., "Nonlocal vibration of carbon nanotubes with attached buckyballs at tip", *Mechanics Research Communications*, 38[1] (2011), pp. 62-67.
17. Chowdhury, R., Adhikari, S. and Scarpa, F., "Vibrational analysis of ZnO nanotubes: A molecular mechanics approach", *Applied Physics A*, 102[2] (2011), pp. 301-308.
18. Chowdhury, R., Adhikari, S., Rees, P., Scarpa, F., and Wilks, S.P., "Graphene based bio-sensor using transport properties", *Physical Review B*, 83[4] (2011), pp. 045401:1-8.
19. Murmu, T. and Adhikari, S., "Axial instability of double-nanobeam-systems", *Physics Letters A*, 375[3] (2011), pp. 601-608.
20. Flores, E. I. S., Adhikari, S., Friswell, M. I. and F. Scarpa, "Hyperelastic finite element model for single wall carbon nanotubes in tension", *Computational Materials Science*, 50[3] (2011), pp. 1083-1087.



References

21. Murmu, T. and Adhikari, S., "Scale-dependent vibration analysis of prestressed carbon nanotubes undergoing rotation", *Journal of Applied Physics*, 108[12] (2010), pp. 123507:1-7.
22. Scarpa, F., Adhikari, S. and Phani, A. Srikanth, "Auxeticity in single layer graphene sheets", *International Journal of Novel Materials*, 1[2] (2010), pp. 39-43.
23. Murmu, T. and Adhikari, S., "Nonlocal effects in the longitudinal vibration of double-nanorod systems", *Physica E: Low-dimensional Systems and Nanostructures*, 43[1] (2010), pp. 415-422.
24. Murmu, T. and Adhikari, S., "Nonlocal transverse vibration of double-nanobeam-systems", *Journal Applied Physics*, 108[8] (2010), pp. 083514:1-9.
25. Scarpa, F., Peng, H. X., Boldri, L., Remillat, C. D. L., Adhikari, S., "Coupled thermo-mechanics of single-wall carbon nanotubes", *Applied Physics Letters*, 97[15] (2010), pp. 151903:1-3.
26. Chowdhury, R., Adhikari, S., Rees, P., "Optical properties of silicon doped ZnO", *Physica B: Condensed Matter*, 405[23] (2010), pp. 4763-4767.
27. Chowdhury, R., Wang, C. W., Adhikari, S. and Scarpa, F., "Vibration and symmetry-breaking of boron nitride nanotubes", *Nanotechnology*, 21[36] (2010), pp. 365702:1-9.
28. Wang, C. Y., Zhao, Y., Adhikari, S. and Feng, Y. T., "Vibration of axially strained triple-wall carbon nanotubes", *Journal of Computational and Theoretical Nanoscience*, 7[11] (2010), pp. 2176-2185.
29. Adhikari, S. and Chowdhury, R., "The calibration of carbon nanotube based bio-nano sensors", *Journal of Applied Physics*, 107[12] (2010), pp. 124322:1-8.
30. Chowdhury, R., Wang, C. Y., Adhikari, S., and Tong, F. M., "Sliding oscillations of multiwall carbon nanotubes", *Physica E: Low-dimensional Systems and Nanostructures*, 42[9] (2010), pp. 2295-2300.



References

31. Chowdhury, R., Adhikari, S., Wang, C. W. and Scarpa, F., "A molecular mechanics approach for the vibration of single walled carbon nanotubes", *Computational Materials Science*, 48[4] (2010), pp. 730-735.
32. Wang, C. Y., Li, C. F., and Adhikari, S., "Axisymmetric vibration of singlewall carbon nanotubes in water", *Physics Letters A*, 374[24] (2010), pp. 2467-2474.
33. Chowdhury, R., Adhikari, S. and Scarpa, F., "Elasticity and piezoelectricity of zinc oxide nanostructure", *Physica E: Low-dimensional Systems and Nanostructures*, 42[8] (2010), pp. 2036-2040.
34. Gil, A. J., Adhikari, S., Scarpa, F., and Bonet, J., "The formation of wrinkles in single layer graphene sheets under nanoindentation", *Journal of Physics: Condensed Matter*, 22[14] (2010), pp. 145302:1-6.
35. Scarpa, F., Adhikari, S. and Chowdhury, R., "The transverse elasticity of bilayer graphene", *Physics Letters A*, 374[19-20] (2010), pp. 2053-2057.
36. Scarpa, F., Adhikari, S., Gil, A. J. and Remillat, C., "The bending of single layer graphene sheets: Lattice versus continuum approach", *Nanotechnology*, 21[12] (2010), pp. 125702:1-9.
37. Chowdhury, R., Rees, P., Adhikari, S., Scarpa, F., and Wilks, S.P., "Electronic structures of silicon doped ZnO", *Physica B: Condensed Matter*, 405[8] (2010), pp. 1980-1985.
38. Scarpa, F., Adhikari, S. and Wang, C. Y., "Nanocomposites with auxetic nanotubes", *International Journal of Smart and Nanomaterials*, 1[2] (2010), pp. 83-94.
39. Chowdhury, R., Wang, C. Y. and Adhikari, S., "Low-frequency vibration of multiwall carbon nanotubes with heterogeneous boundaries", *Journal of Physics D: Applied Physics*, 43[11] (2010), pp. 085405:1-8.
40. Chowdhury, R., Adhikari, S. and Mitchell, J., "Vibrating carbon nanotube based bio-sensors", *Physica E: Low-dimensional Systems and Nanostructures*, 42[2] (2009), pp. 104-109.



References

41. Scarpa, F., Adhikari, S. and Wang, C. Y., "Mechanical properties of non reconstructed defective single wall carbon nanotubes", *Journal of Physics D: Applied Physics*, 42 (2009) 142002 (6pp).
42. Wang, C. Y., Li, C. F., and Adhikari, S., "Dynamic behaviors of microtubules in cytosol", *Journal of Biomechanics*, 42[9] (2009), pp. 1270-1274.
43. Tong, F. M., Wang, C. Y., and Adhikari, S., "Axial buckling of multiwall carbon nanotubes with heterogeneous boundary conditions", *Journal of Applied Physics*, 105 (2009), pp. 094325:1-7.
44. Scarpa, F., Adhikari, S. and Phani, A. Srikanth, "Effective mechanical properties of single graphene sheets", *Nanotechnology*, 20[1-2] (2009), pp. 065709:1-11.
45. Scarpa, F. and Adhikari, S., "Uncertainty modelling of carbon nanotube terahertz oscillators", *Journal of Non-Crystalline Solids*, 354[35-39] (2008), pp. 4151-4156.
46. Scarpa, F. and Adhikari, S., "A mechanical equivalence for the Poisson's ratio and thickness of C-C bonds in single wall carbon nanotubes", *Journal of Physics D: Applied Physics*, 41 (2008) 085306 (5pp).